

2012

NEW METRICS FOR SPACE-TIME DECODING WITH IMPERFECT SYNCHRONIZATION

GARIMA DEEP

University of Windsor

Follow this and additional works at: <http://scholar.uwindsor.ca/etd>

Recommended Citation

DEEP, GARIMA, "NEW METRICS FOR SPACE-TIME DECODING WITH IMPERFECT SYNCHRONIZATION" (2012).
Electronic Theses and Dissertations. Paper 120.

This online database contains the full-text of PhD dissertations and Masters' theses of University of Windsor students from 1954 forward. These documents are made available for personal study and research purposes only, in accordance with the Canadian Copyright Act and the Creative Commons license—CC BY-NC-ND (Attribution, Non-Commercial, No Derivative Works). Under this license, works must always be attributed to the copyright holder (original author), cannot be used for any commercial purposes, and may not be altered. Any other use would require the permission of the copyright holder. Students may inquire about withdrawing their dissertation and/or thesis from this database. For additional inquiries, please contact the repository administrator via email (scholarship@uwindsor.ca) or by telephone at 519-253-3000ext. 3208.

NEW METRICS FOR SPACE-TIME DECODING
WITH IMPERFECT SYNCHRONIZATION

by

Garima Deep

A Thesis

Submitted to the Faculty of Graduate Studies
through Electrical and Computer Engineering
in Partial Fulfillment of the Requirements for
the Degree of Master of Applied Science at the
University of Windsor

Windsor, Ontario, Canada

2012

© 2012 Garima Deep

NEW METRICS FOR SPACE-TIME DECODING
WITH IMPERFECT SYNCHRONIZATION

by

Garima Deep

APPROVED BY:

Dr. Robin Gras
School of Computer Science

Dr. Majid Ahmadi
Department of Electrical and Computer Engineering

Dr. Behnam Shahrrava
Department of Electrical and Computer Engineering

Dr. Mitra Mirhassani
Chair of Defense

13 June, 2012

Declaration of Previous Publications

This thesis includes 2 original papers that have been previously submitted for publication in peer reviewed journals and conferences, as follows:

Thesis Chapter	Publication title/full citation	Publication status
Chapter 5	G. Deep, B. Shahrava, S. Sinha “Space-Time Decoding with Imperfect Synchronization”; IEEE International Global Telecommunication Conference	submitted
Chapter 5	G. Deep, B. Shahrava, S. Sinha “Optimal Space-Time Decoding with Imperfect Synchronization”; 2012 IEEE Workshop on Signal Processing Systems	submitted

I certify that I have obtained a written permission from the copyright owner(s) to include the above published material(s) in my thesis. I certify that the above material describes work completed during my registration as graduate student at the University of Windsor.

I declare that, to the best of my knowledge, my thesis does not infringe upon anyones copyright nor violate any proprietary rights and that any ideas, techniques, quotations, or any other material from the work of other people included in my thesis, published or otherwise, are fully acknowledged in accordance with the standard referencing practices. Fur-

thermore, to the extent that I have included copyrighted material that surpasses the bounds of fair dealing within the meaning of the Canada Copyright Act, I certify that I have obtained a written permission from the copyright owner(s) to include such material(s) in my thesis.

I declare that this is a true copy of my thesis, including any final revisions, as approved by my thesis committee and the Graduate Studies office, and that this thesis has not been submitted for a higher degree to any other University or Institution.

Co-Authorship Declaration

I hereby declare that this thesis incorporates material that is result of joint research, as follows:

This thesis also incorporates the outcome of a joint research undertaken in collaboration with Shayondip Sinha under the supervision of professor Dr. Behnam Shahrava. The collaboration is covered in Chapter 5 of the thesis. In all cases, the key ideas, primary contributions, experimental designs, data analysis and interpretation, were performed by the author, and the contributions of co-authors were primarily through the provision of proof reading and reviewing the research papers regarding the technical content.

I am aware of the University of Windsor Senate Policy on Authorship and I certify that I have properly acknowledged the contribution of other researchers to my thesis, and have obtained written permission from each of the co-authors to include the above materials in my thesis.

I certify that, with the above qualification, this thesis, and the research to which it refers, is the product of my own work.

Abstract

This thesis emphasizes the unexploited challenges in an unsynchronized space-time block coded (STBC) system. This research involves the unknown Rayleigh fading channel parameters and the carrier frequency offset (CFO) at the receiver. Plenty of research has been done on the optimal estimation of these parameters over the period of time. Considering a practical receiver system with a non-ideal estimator leads to the necessity of introducing the erroneous estimates of these unknown parameters into the detection algorithm. It is therefore necessary to augment the existing conventional detectors, such as maximum likelihood (ML), maximal ratio combiner (MRC) and minimum mean square error (MMSE). This work is an extension of these conventional detection schemes, which will make the proposed detectors capable of overcoming the challenge of mismatch scenario. The proposed detectors are designed to optimize the output at the receiver, for various estimation error variances of the uncertainties. Extensive simulation results demonstrate that the proposed schemes outperform conventional detectors. The performance of these proposed detectors is analyzed by plotting the bit error rate (BER) over signal to noise ratio (SNR) curves for various modulation schemes, such as M-PSK and M-QAM. At the end, the computational complexities of the proposed detectors from the implementation point of view is discussed briefly.

to my family

Acknowledgements

Firstly, I would like to thank my advisor, Dr. Behnam Shahrava, for his guidance and constant support throughout my Masters program. He has been an excellent guide who developed my interest in research and demonstrated concern for every complication I faced during this research work. His insight on the subject and comments were invaluable and it was a pleasure to work with him.

I would like to express my gratitude to Dr. Robin Gras and Dr. Majid Ahmadi for giving me valuable feedback and for their time spent serving my graduate committee. I would also like to express my deep gratitude to Dr. Nihar Biswas for his extended help and willingness to offer advice at each step along the way. My special thanks to the departmental staffs, particularly, Ms. Andria Ballo, Ms. Shelby Marchand and Mr. Frank Cicchello for their support and for providing me an excellent work environment.

I feel highly gratified towards my friends Ashirbani Saha, Dibyendu Mukherjee, Dr. Gaurav Bhatnagar and Shayondip Sinha for all the help they provided, the knowledge they shared and the resources they made available, without which the research would not have been this successful.

My motivation is my grandfather who taught me to work hard and reach higher. His love and affection encouraged me to complete my research early so that I could spend more time with him afterwards. I could not be where I am today, without the unconditional love

and encouragement of my '*chachijis*,' who never let me feel away from mom and home, my '*chachajis*,' who walked those extra miles to make sure I was safe and my cousin brothers, who made me feel like a princess in their empire.

I owe this all to my parents and my brother, who were beside me at every step. Their daily phone calls to ask my progress in research and to keep me connected with the almighty, helped me in every aspect, which I will never forget. I feel their dreams are going to come true and their prayers seem to be answered.

Finally, I would like to thank my '*mamaji*,' for his constant encouragement to attain higher education and make my family feel proud of me.

Above all, the success of my work make me feel, the presence of my late grandma and her blessings being showered on me.

Thank you, Lord, for wonderful, priceless family and friends.

Table of Contents

	Page
Declaration of Previous Publications	iii
Co-Authorship Declaration	v
Abstract	vi
Acknowledgements	viii
List of Tables	xiv
List of Figures	xv
List of Acronyms	xvii
Glossary of Symbols	xix
1 Introduction	1
1.1 Transmitter Module	2
1.1.1 Modulation Techniques	2
1.1.1.1 M-QAM	3
1.1.1.2 M-PSK	4
1.1.2 Diversity Schemes	5
1.1.2.1 Time Diversity	7
1.1.2.2 Frequency Diversity	7
1.1.2.3 Phase Diversity	7
1.1.2.4 Code Diversity	7
1.1.2.5 Space Diversity	8
1.1.3 Space Antenna Diversity	8

1.1.3.1	SISO	8
1.1.3.2	SIMO	8
1.1.3.3	MISO	9
1.1.3.4	MIMO	9
1.2	Channel Module	10
1.2.1	Channel State Information	11
1.2.2	AWGN	11
1.3	Receiver Module	12
1.3.1	Synchronized Receiver	13
1.3.2	Unsynchronized Receiver	14
1.4	Objective of the Research	15
1.5	Structure of the Thesis	16
2	Literature Review	18
3	Space-Time Block Coding	21
3.1	Introduction	21
3.2	STBC System Model	22
3.2.1	STBC Transmitter	23
3.2.2	STBC Receiver	24
3.2.2.1	MRC combiner scheme	25
3.2.2.2	ML decision scheme	26
3.3	Effect of parameter estimation errors	27
3.3.1	System model with unknown CSI	27
3.3.1.1	Simulation performance of unknown CSI	29
3.3.2	System model with unknown CFO	33
3.3.2.1	Simulation performance of unknown CFO	35
4	STBC detection techniques	39
4.1	Maximum Likelihood detector	40
4.1.1	ML System discription	40

4.1.2	ML detector with unknown CSI based upon CEP	42
4.1.3	ML detector with unknown CSI & CFO based upon CEP	43
4.2	Maximal Ratio Combiner and ML detection scheme	44
4.2.1	MRC System discription	45
4.2.2	MRC detector with unknown CSI based upon CEP	46
4.2.3	MRC detector with unknown CSI & CFO based upon CEP	48
4.3	Minimum Mean Square Error detector	49
4.3.1	MMSE System discription	50
4.3.2	MMSE detector with unknown CSI based upon CEP	52
4.3.3	MMSE detector with unknown CSI & CFO based upon CEP	53
5	Proposed detection schemes based upon the unknown CSI and CFO estimation errors	55
5.1	Overview	55
5.2	Assumptions	57
5.3	Proposed ML detector	58
5.3.1	Convergence to conventional ML detector	60
5.4	Proposed MRC detector	61
5.4.1	ML Detection Methodology	63
5.4.2	Convergence to conventional MRC detector	63
5.5	Proposed MMSE detector	64
5.5.1	Convergence to conventional MMSE detector	66
5.6	Simulation analysis	67
6	Conclusion and Future Work	75
	References	77
	Appendix	
A	Mathematical Calculations	87
A.1	Conditional PDF of CAFO	87
A.2	Conditional Expectation of CAFO	89

A.3	Conditional Expectation of Received Signal	90
A.4	Conditional Variance of Received Signal	91
Vita Auctoris	93

List of Tables

3.1	Data transmission	23
3.2	CFO distribution with channel and time	33

List of Figures

1.1	Generic block diagram of wireless communication system.	2
1.2	Signal space diagram of QAM modulations.	3
1.3	Signal space diagram of PSK modulations.	4
1.4	Diversity Schemes.	6
1.5	Types of Space/Antenna Diversity.	9
1.6	Multipath fading in wireless communication system.	10
1.7	Modulation Block Diagram	12
1.8	Synchronized demodulation	13
1.9	Unsynchronized demodulation	14
3.1	Space Time Coding.	21
3.2	Space Time Block Coding transmitter.	23
3.3	Space Time Block Coding receiver.	24
3.4	Performance of 4-PSK STBC system for different pilot length.	30
3.5	Performance of M-PSK STBC system for different pilot length.	31
3.6	Performance of M-QAM STBC system for different pilot length.	32
3.7	Performance of unsynchronized 4-PSK STBC system under mismatch scenario.	35
3.8	Performance of unsynchronized M-PSK STBC system under mismatch scenario.	36

3.9	Performance of unsynchronized 4-QAM STBC system under mismatch scenario.	37
3.10	Performance of unsynchronized M-QAM STBC system under mismatch scenario.	38
4.1	An ideal ML detector receiver	40
4.2	An ML detector with unknown CSI estimates	42
4.3	An unsynchronized ML detector with unknown CSI estimates	43
4.4	An ideal MRC detector receiver	45
4.5	An MRC detector with unknown CSI estimates	47
4.6	An unsynchronized MRC detector with unknown CSI estimates	48
4.7	An ideal MMSE detector receiver	49
4.8	Vector diagram of MSE	50
4.9	An MMSE detector with unknown CSI estimates	52
4.10	An unsynchronized MMSE detector with unknown CSI estimates	53
5.1	Performance of 4-PSK STBC system with proposed detector.	69
5.2	Performance of 4-PSK STBC system with proposed detector.	70
5.3	Performance of M-PSK STBC system with proposed detector.	71
5.4	Performance of 4-QAM STBC system with proposed detector.	72
5.5	Performance of M-QAM STBC system with proposed detector.	73

List of Acronyms

AWGN	Additive White Gaussian Noise
AM	Amplitude Modulation
BER	Bit Error Rate
BS	Base Station
CAFO	Carrier Angular Frequency Offset
CEP	Certainty Equivalence Principle
CFO	Carrier Frequency Offset
CSI	Channel State Information
iid	Independent and Identically Distributed
ICI	Inter Carrier Interference
LTE	Long Term Evolution
MA	Multiple Antenna
MIMO	Multiple Input Multiple Output
MISO	Multiple Input Single Output

ML	Maximum Likelihood
MSE	Mean Square Error
MMSE	Minimum Mean Square Error
MRC	Maximal Ratio Combining
O-PSI	Orthogonal Pilot Sequence Insertion
PSK	Phase Shift Keying
QAM	Quadrature Amplitude Modulation
RU	Remote Unit
RV	Random Variable
SED	Squared Euclidean Distance
SIMO	Single Input Multiple Output
SISO	Single Input Single Output
SNR	Signal-to-Noise Ratio
STBC	Space-Time Block Coding
STC	Space-Time Codes
STTC	Space-Time Trellis Codes
WC	Wireless Communication

Glossary of Symbols

$[\cdot]^T$	Transpose of a vector or matrix
$[\cdot]^*$	Complex conjugate of a vector or matrix
$[\cdot]^H$	Hermitian of a vector or matrix
$\ \cdot\ $	Euclidean norm
$\Re\{\cdot\}$	Real value of a variable
\perp	Orthogonal
\ln	Natural logarithm
$E[\cdot]$	Expected value of a random variable
$Var[\cdot]$	Variance of a random variable
$P(x)$	Probability of the occurrence of x
j	$\sqrt{-1}$
$f(\cdot)$	Probability density function
$A \sim \mathcal{N}(\mu, \sigma_A^2)$	A is a Gaussian random variable with mean μ and variance σ_A^2

Chapter 1

Introduction

Today, Wireless Communication has a significant impact on everyone's life. The development of the endless enabling technologies like advanced mobile phones with digital cameras, wireless internet, television, radios etc. keep us connected and provide us with all sort of information from all around the world. With the evolution of these rapidly developing crucial technologies, wireless communication (WC) became an indispensable field of research. To cope up with increasing demands for simple, highly efficient and unified technology, the main objective is to have a quality and reliable transmission of the signal. With the increasing number of end-users, the obstacle ahead is the restriction on limited bandwidth. Researchers from all around the world are constantly exploring the techniques for bandwidth extension and spectrum aggregation. Some emerging nations have adopted the advanced wireless communication 4G Long Term Evolution (LTE) technology, which promises to cater the ever increasing data rate demand.

To understand the fundamental concept of WC system Fig. 1.1 shows a general block diagram of a WC system which can be broadly modeled as, implicit transmission of information signal propagating on the physical medium called channel and its reconstruction to a recognizable form at the receiver.

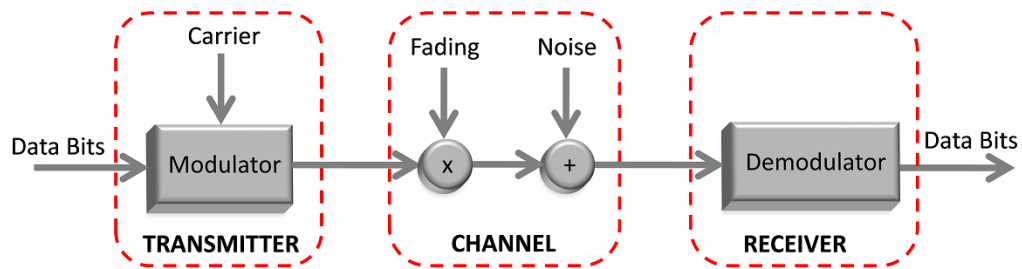


Figure 1.1: Generic block diagram of wireless communication system.

1.1 Transmitter Module

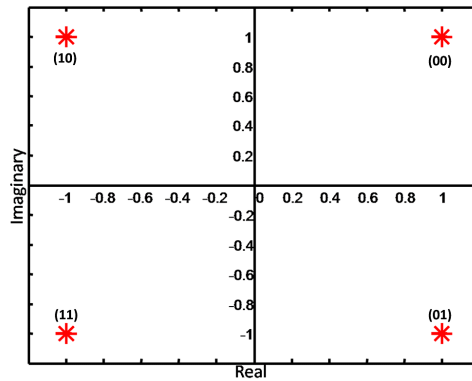
The main characteristic of a transmitter is to modify the data bits into an electric signal referred as baseband signal. The baseband signal is then processed to ease its transmission through the channel. These signal processing involves amplification, modulation on a high frequency carrier wave etc. for efficient transmission.

1.1.1 Modulation Techniques

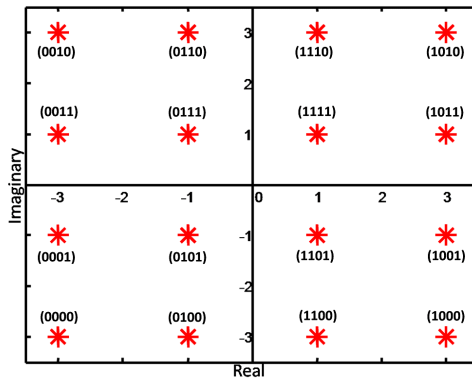
Modulation, the fundamental block of communication is defined as a process which involves varying some parameter of the carrier signal in accordance to the instantaneous value of the baseband signal for suitable transmission over the channel [1]. In the new era, digital communication is used for its tremendous advantages over the analog communication. In digital communication, the modulator maps the input binary codeword to analog carrier signal for transmission. There are many modulation schemes [2,3] currently employed on WC system. The work presented in this thesis is on the major modulation schemes used recently i.e.

1.1.1.1 M-QAM

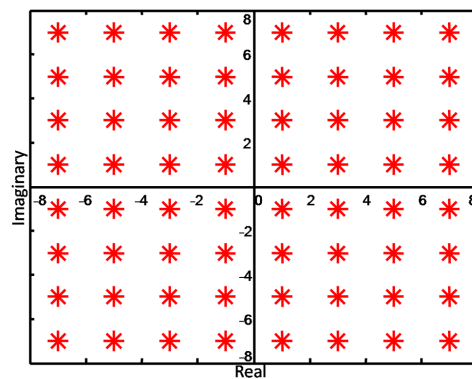
Amplitude modulation (AM) is defined as a system in which the amplitude of the continuous carrier wave is varied in accordance to the instantaneous amplitude of the baseband signal [4]. Thus, the unique property of AM wave is that, its frequency and phase remains constant however, the varying envelop of the modulated carrier wave contains all the information of the baseband signal. Quadrature amplitude modulation (QAM) can be done in various rates [5] as shown in 1.2. Taking advantage of its remarkable performance [6–8] in various systems, it has proved to be one of the most popular methods employed for high technology wireless systems [9, 10].



(a) 4-QAM modulation



(b) 16-QAM modulation

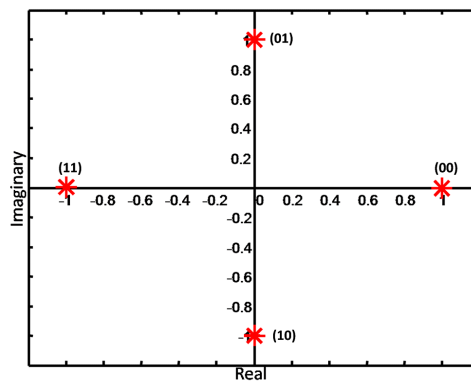


(c) 64-QAM modulation

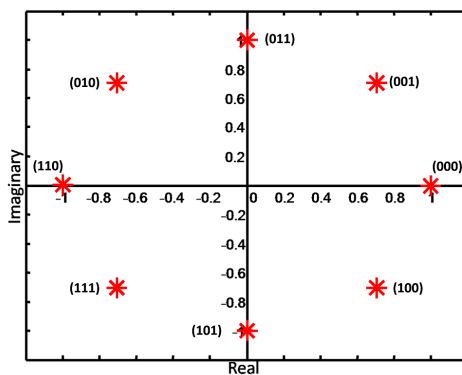
Figure 1.2: Signal space diagram of QAM modulations.

1.1.1.2 M-PSK

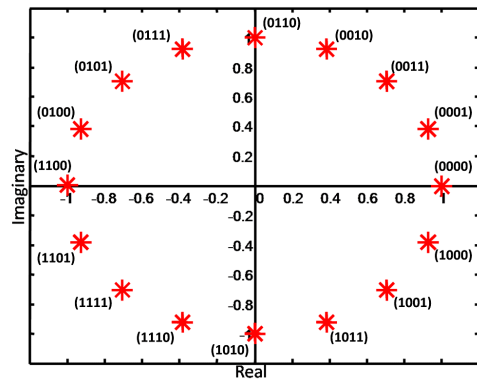
In digital communication, when the modulation process involves switching or keying the phase of the high frequency carrier wave in accordance to the digital baseband signal, this process is called Phase Shift Keying (PSK). PSK has a constant envelop and varying phase hence is less prone to external interferences, contrary to AM which is more pronounced to external noise. The performance of PSK in WC system has been vastly done in [11–14] for various areas of interest. Figure. 1.3 shows various PSK modulation techniques used in this research for studying the system performance.



(a) 4-PSK modulation



(b) 8-PSK modulation



(c) 16-PSK modulation

Figure 1.3: Signal space diagram of PSK modulations.

Modulation has proved to be of tremendous importance in WC. The quality of transmission lies in higher signal to noise ratio. The lower modulation schemes work well on lower SNR. However, they have lower data rate. Although, the higher order modulation schemes require higher SNR for optimal transmission, its unduly advantage is its higher data rates.

The higher modulation indexes have advantages over the lower as:

- The bandwidth for M-modulation schemes is M times less as compared to the lower modulation schemes for same BER.
- Due to the reduced bandwidth, the bit transmission rate is higher for higher modulation schemes

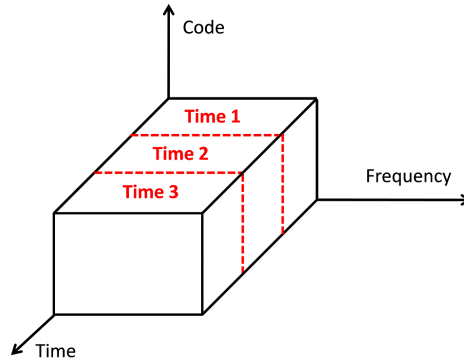
There has been enormous research done for the best modulation scheme [15–18]. It all depends upon the required data rate, transmission medium and fading in the channel.

1.1.2 Diversity Schemes

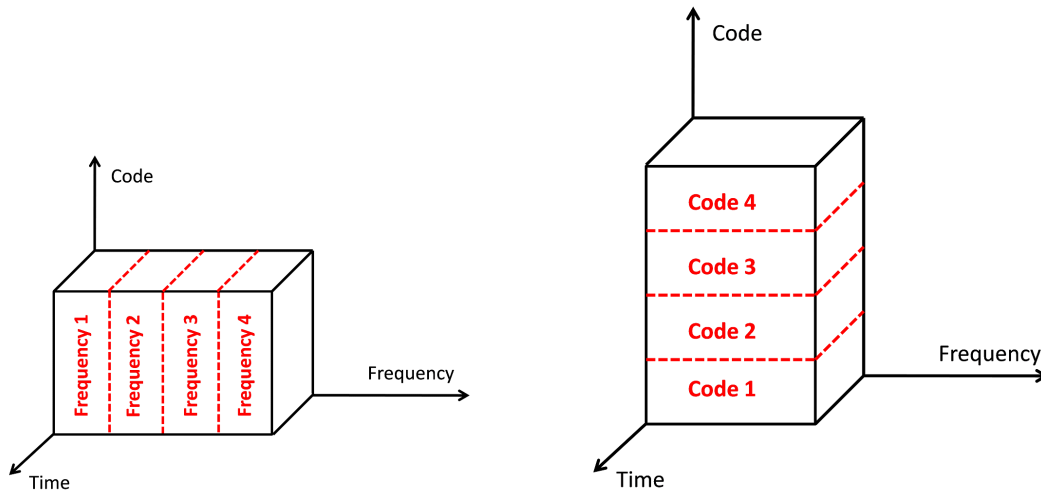
In Wireless Communication world, the main objective is to have a quality and reliable transmission of the signal. However due to adverse weather conditions, variation in time, geographical regions etc., it is very difficult to have an incorrupt speech or data signal. As mentioned below, another major challenge of WC system is the uncertain channel coefficients. The transmitted signal propagates from a multipath channel, where the signal fluctuates over a period of time or distance transverse. Multipath propagation gives rise to inter carrier interference (ICI) and degrades the system performance, which is termed as 'fading'. This thesis emphasizes on multipath fading, which imposes difficulties in optimum reception of the baseband signal.

Diversity is a technique to mitigate the effect of fading and ICI [19, 20]. 'Diversity' in other words can be defined as, sending different replicas of the same transmitted signal to

the receiver over different channels, so that it becomes more probable to detect the original signal. There are several classes of diversity schemes employed at the transmitter for more reliable signal reception.



(a) Time Diversity



(b) Frequency Diversity

(c) Code Diversity

Figure 1.4: Diversity Schemes.

1.1.2.1 Time Diversity

Time diversity is the most common diversity where redundant data are time interleaved so that they experience independent fades. An error correcting code added to the signal simplifies the error and avoids error bursts.

1.1.2.2 Frequency Diversity

In Frequency diversity, redundant data symbols are transmitted over multiple frequency bands. The different carrier frequencies are selected in such a way so that each individual data symbol on a carrier experience independent fading.

1.1.2.3 Phase Diversity

The broadband signal is processed in a similar way as the frequency diversity. However, in phase diversity, the different replicas of the same baseband signal are modulated over the carrier with different phases. In this diversity scheme, the time and frequency are constant over the channel. The receiver oscillator is tuned to the different phases of the carrier to demodulate the baseband signal with less probably to lose the original data due to different multipath fading.

1.1.2.4 Code Diversity

Code diversity provides improved system performance by encoding the baseband signal to specific code sequences before modulating it on the carrier. On the receiver side, the signal is demodulated and the encoded data is decoded into its original form. In this way, code diversity provides security and higher coding gain without any bandwidth expansion. The effectiveness of code diversity to combat fading made it evolve remarkably with the evolution of time.

1.1.2.5 Space Diversity

Space diversity is an effective diversity technique [21–23] where multiple transmitters and/or multiple receiver antennas are employed to transmit the replicas of the baseband signal. Multiple antennas ensure independent fading across different channels. The receiver combines the multipath signal to reconstruct the optimal baseband signal. The space diversity is also known as antenna diversity. There are other diversity schemes like angular diversity where redundant data is send over directional antennas, polarization diversity where the advantage of antenna polarization is taken to achieve diversity, etc.

1.1.3 Space Antenna Diversity

Space/Antenna Diversity can be categorized as:

1.1.3.1 SISO

Single-input single-output antenna is a basic communication model with one transmitter and one receiver. SISO does not employ antenna diversity technique. Today, SISO models are used to compare the performance of antenna diversity schemes over the basic WC system.

1.1.3.2 SIMO

Single-input multiple-output antenna diversity holds for a system with single transmitter and multiple receivers. SIMO is the most primitive technique also termed as receiver diversity [24, 25]. In SIMO, receiver effectively combines the multiple copies of the same transmitted signal over multiple channels to maximize the SNR of the output signal. Consideration the demand is of a simple, highly efficient, pocket remote unit (RU), SIMO technique is applied in the uplink of a WC system with single antenna at the RU and multiple antennas at the base station (BS) [26–28].

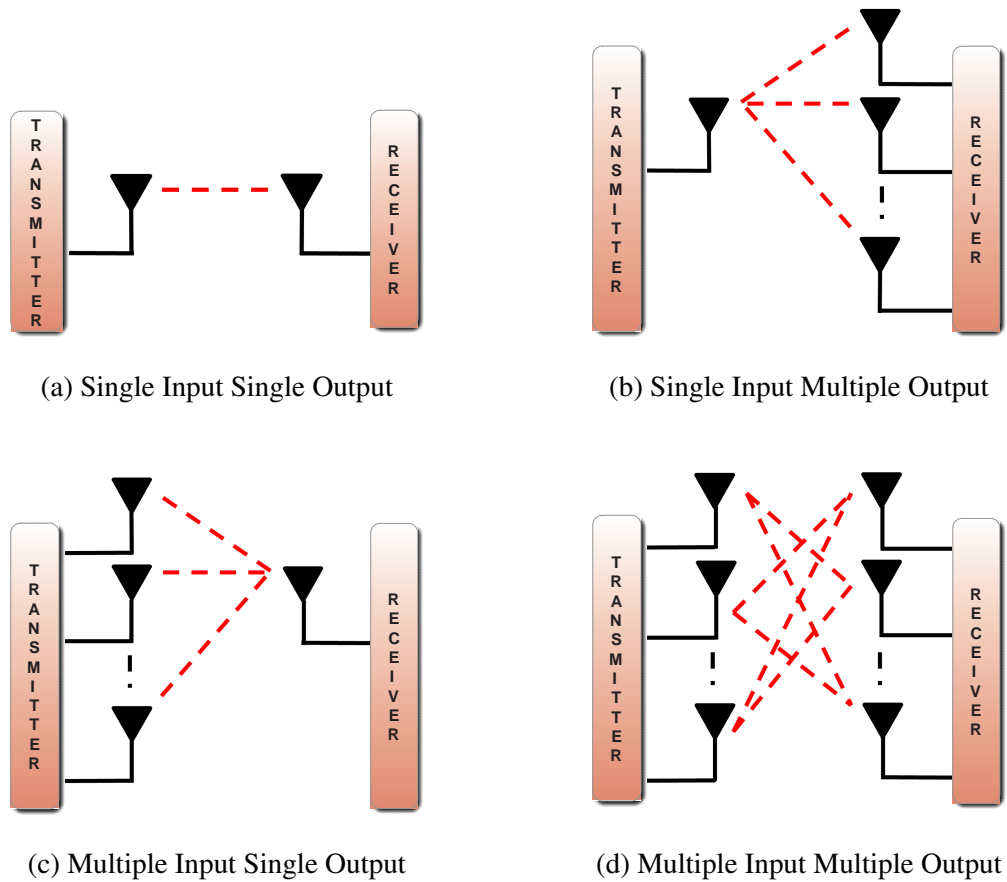


Figure 1.5: Types of Space/Antenna Diversity.

1.1.3.3 MISO

Multiple-input single-output antenna diversity employs multiple antennas at the transmitter and single antenna at the receiver. MISO diversity has been exploited recently and is also termed as transmitter diversity [29–31]. This scheme is employed in the downlink of a WC system, with single antenna at receiver to keep it light and less complex.

1.1.3.4 MIMO

Multiple input multiple output (MIMO) system exploits the advantage of having multiple antennas at both transmitter and the receiver [32, 33]. MIMO is also known as smart

antenna technology. While MIMO systems account more complexity at both transmitter and receiver, however, its proficient signal processing algorithms provide better quality of transmission and support superior data transfer rates [34–36] as compared to the traditional SISO antenna system.

1.2 Channel Module

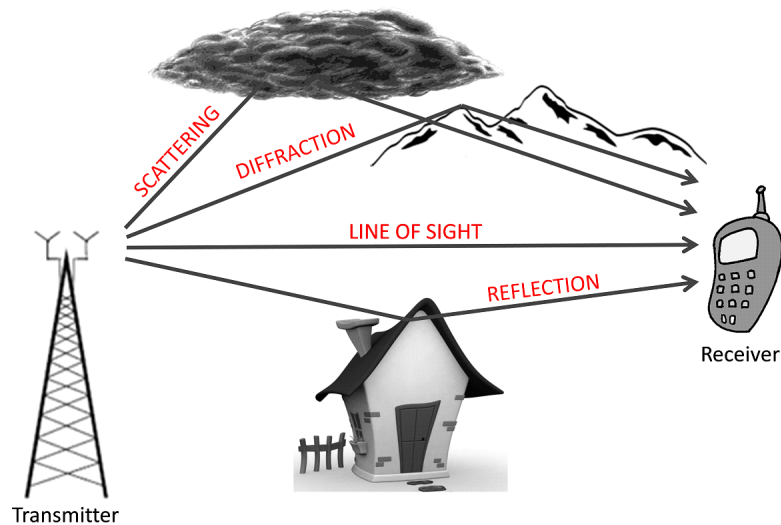


Figure 1.6: Multipath fading in wireless communication system.

As shown in the block diagram in Fig. 1.1, channel is a medium through which the electrical signals propagate from transmitter to the receiver. In real sense, channel is a filter which attenuates and deteriorates the transmitted signal. Fig. 1.6 demonstrates how a signal propagate after scattering, reflecting, refracting, deflecting in a practical scenario. The received signal is not a mere line of sight, but copies of multipath transmissions encountered from different directions, time and energy. Thus the unpredictable channel makes the WC communication system very complex.

1.2.1 Channel State Information

The channel plays an important role in designing communication system. There are various types of fading channels and a survey of their error performance is done in [37]. In this thesis, we will examine the impact of Rayleigh fading in the mobile radio channel on the transmitted signal [38].

As given in [39], the received signal rapidly fluctuates in space, time or frequency domain and scatters due to the interfering objects in between the transmitter and the receiver. Rayleigh Fading applies to the case when no dominant signal propagated along the line of sight. Thus, the received signal is a superposition of all the scattered faded signals. Hence, by central limit theorem [40], Rayleigh channel is characterized as a random variable whose real and imaginary parts are zero mean independent and identically distributed (IID) Gaussian variables with equal variance.

$$h_i = \alpha_i e^{j\theta_\alpha} \quad (1.1)$$

Where α_i is the amplitude of the i^{th} sinusoid which is a constant of 1 in our case, θ_α is the random phase uniformly distributed from zero to 2π . Therefore, the envelope of the received signal follows a Rayleigh distribution with following pdf:

$$f_H(h) = \frac{h}{\sigma^2} e^{\left(\frac{-h^2}{2\sigma^2}\right)} \quad (1.2)$$

where σ^2 is the variance of the channel coefficient. Channel fading is also caused by motion of the receiver. This movement introduces Doppler Shift in the received signal, which is the relative change in the frequency of the propagating signal due to the motion of the receiver.

1.2.2 AWGN

Noise is another important factor that has tremendous impact on the signal. Noise is an unwanted, unpredictable, random interference which distorts the signal and cannot be compensated for. In digital communications, signal power decreases with increasing distance

over a channel. SNR is a measurement which is defined as signal power to the noise power. Thus, lower noise maintains higher SNR, enabling successful data transmission over the wireless channel. Whereas, higher noise demolishes SNR and distorts the signal to an extent, that cannot be recovered accurately at the receiver.

In addition to the multiplicative channel coefficient, this noise is considered an additive counterpart of the final received signal in every wireless communication system. The noise is considered a random variable with Gaussian distribution and a flat power spectral density over the bandwidth of the signal. Thus, it is categorized as additive white Gaussian noise (AWGN).

1.3 Receiver Module

As explained above, the transmitter's primary purpose is to deliver the message signal to the receiver. For an accurate transmission of the information signal, transmitter modulates the baseband signal to make it suitable for transmitting over the channel. Similarly, the receiver demodulates the received signal to recreate the baseband signal. Thus, the receiver circuit is most important for an optimal detection of the signal. The following section demonstrates the mathematical calculations for the demodulation of the two receivers with synchronized carrier oscillator and unsynchronized oscillator.

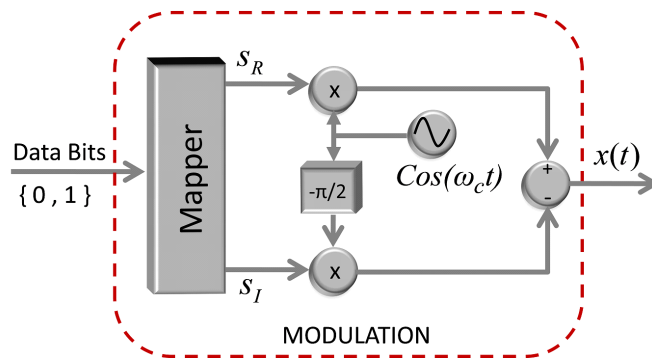


Figure 1.7: Generic block diagram of modulation in wireless communication system.

Block diagram in Fig. 1.7 demonstrates how a complex baseband signal is modulated over the high frequency carrier wave. Depending on different modulation schemes, the complex baseband signal is mapped to a form $s = s_R + js_I$. The baseband signal is then modulated with a carrier wave of frequency f_c . Thus the radio frequency (RF) signal transmitted from the antenna can be given by

$$\begin{aligned} x(t) &= \Re \{ s e^{j\omega_c t} \} \\ &= \Re \{ (s_R + js_I) (\cos(\omega_c t) + j \sin(\omega_c t)) \} \\ &= s_R \cos(\omega_c t) - s_I \sin(\omega_c t), \end{aligned} \quad (1.3)$$

where $\omega_c = 2\pi f_c$.

1.3.1 Synchronized Receiver

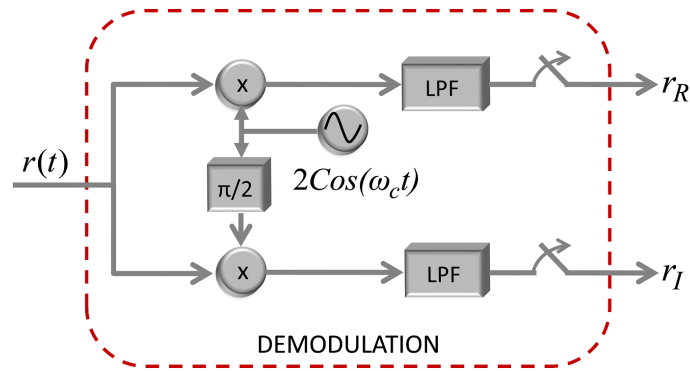


Figure 1.8: Generic block diagram of synchronized demodulation in wireless communication system.

In ideal scenario, the oscillator of the receiver should be in synchronization with the same carrier frequency f_c as that of the transmitter, as shown in Fig. 1.8. The RF signal at the receiver is of the form

$$r(t) = r_R \cos(\omega_c t) - r_I \sin(\omega_c t). \quad (1.4)$$

The demodulation of the received signal at branch one becomes,

$$\begin{aligned} 2r(t) \cos(\omega_c t) &= 2r_R \cos^2(\omega_c t) - 2r_I \sin(\omega_c t) \cos(\omega_c t) \\ &= r_R \{\cos(2\omega_c t) + 1\} - r_I \{\sin(2\omega_c t)\}. \end{aligned} \quad (1.5)$$

It is then passed through a low pass filter and the output is r_R . Similarly, in branch two

$$\begin{aligned} -2r(t) \sin(\omega_c t) &= -2r_R \cos(\omega_c t) \sin(\omega_c t) + 2r_I \sin^2(\omega_c t) \\ &= -r_R \{\sin(2\omega_c t)\} + r_I \{1 - \cos(2\omega_c t)\}. \end{aligned} \quad (1.6)$$

This is also passed through a low pass filter with an output r_I . The signal is further sampled to obtain the digital baseband signal.

1.3.2 Unsynchronized Receiver

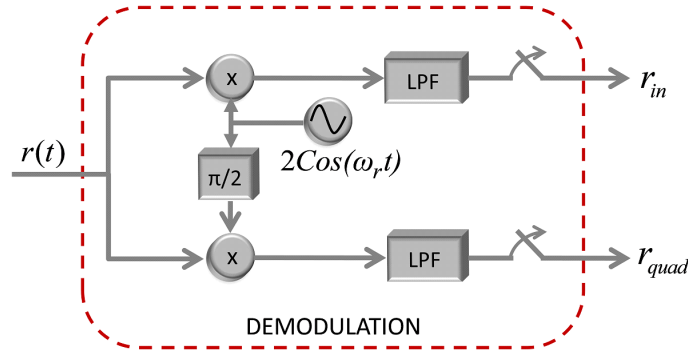


Figure 1.9: Generic block diagram of unsynchronized demodulation in wireless communication system.

As discussed above, in order to perfectly retrieve the baseband signal, the oscillator frequency of the receiver should be ideally tuned to the carrier frequency. However in practical scenario, the two frequencies differ. This happens due to varied reasons like Doppler shifts or device impairment causing physical differences between the local oscillators of transmitter and receiver. When the receiver's oscillator frequency is unsynchronized with the carrier frequency, as shown in Fig. 1.9, the difference in the frequency is known as CFO.

CFO introduces ICI by destroying the orthogonality between the carriers and thus causes acute reduction in SNR. Thus, CFO has to be estimated at the receiver because it deteriorates the performance of the system during demodulation, which can be expressed in the form

$$\begin{aligned}\Delta\omega &= \omega_c - \omega_r \\ \Rightarrow 2\pi\Delta f &= 2\pi f_c - 2\pi f_r,\end{aligned}\tag{1.7}$$

where Δf is the CFO which is a difference between f_c , the carrier frequency and f_r , the frequency of the receiver oscillator. The demodulation of the received signal at branch one becomes,

$$\begin{aligned}2r(t) \cos(\omega_r t) &= 2 r_R [\cos^2(\omega_c t) \cos(\Delta\omega t) + \cos(\omega_c t) \sin(\omega_c t) \sin(\Delta\omega t)] \\ &\quad - 2 r_I [\sin(\omega_c t) \cos(\omega_c t) \cos(\Delta\omega t) + \sin^2(\omega_c t) \sin(\Delta\omega t)] \\ &= r_R [\{1 + \cos(2\omega_c t)\} \cos(\Delta\omega t) + \sin(2\omega_c t) \sin(\Delta\omega t)] \\ &\quad - r_I [\sin(2\omega_c t) \cos(\Delta\omega t) + \{1 - \cos(2\omega_c t)\} \sin(\Delta\omega t)].\end{aligned}\tag{1.8}$$

It is then passed through a low pass filter and the in-phase output r_{in} is $r_R \cos(\Delta\omega t) - r_I \sin(\Delta\omega t)$. Similarly, in branch two

$$\begin{aligned}-2r(t) \sin(\omega_r t) &= - 2 r_R [\cos(\omega_c t) \sin(\omega_c t) \cos(\Delta\omega t) - \cos^2(\omega_c t) \sin(\Delta\omega t)] \\ &\quad + 2 r_I [\sin^2(\omega_c t) \cos(\Delta\omega t) - \sin(\omega_c t) \cos(\omega_c t) \sin(\Delta\omega t)] \\ &= - r_R [\sin(2\omega_c t) \cos(\Delta\omega t) - \{1 + \cos(2\omega_c t)\} \sin(\Delta\omega t)] \\ &\quad + r_I [\{1 - \cos(2\omega_c t)\} \cos(\Delta\omega t) - \sin(2\omega_c t) \sin(\Delta\omega t)].\end{aligned}\tag{1.9}$$

This is also passed through a low pass filter with the quadrature-phase output r_{quad} as $r_R \sin(\Delta\omega t) + r_I \cos(\Delta\omega t)$. The signal thus contain a carrier frequency offset term, which does not allow an optimal detection of the baseband signal and has to be removed.

1.4 Objective of the Research

An optimum reception of the baseband signal is of great importance for mainly two reasons in a multiple antenna (MA) WC system. Firstly, in a MA system, there are multiple

copies of the transmitted signal through multiple unknown channels with different powers and degradations. Ideal detection algorithms are designed with an assumption that the CSI is perfectly known to the receiver. However, practical systems require estimating the channel fading parameters before detection of the baseband signal. Besides unknown channel parameters, in a MA system, the propagation of baseband signal through multipaths can undergo co-channel interference or even loss of data due to Doppler shift. Doppler shift or even oscillators impairments can introduce CFO which is unavoidable in an unsynchronized system.

This research examines all the problems discussed above and focuses on designing detectors at the receivers. The aim is to achieve optimal detection of the multiple transmissions of the message signal through a flat Rayleigh fading environment and addition of AWGN noise. To supersede the effect of interference, space-time block coding (STBC) scheme (discussed in Chapter 3) is used to maintain orthogonality between the baseband signals transmitted over multiple antennas. The detectors are modeled under combined impairments of imperfect CSI and CFO. The algorithms are designed for three prevalent detection techniques, incorporating the estimation error variances associated with the estimates of channel fading parameters and CFO. Simulations are performed and analyzed in terms of BER for various proposed detectors, which outperform in comparison to the conventional detection techniques.

1.5 Structure of the Thesis

The rest of the thesis is organized as follows.

Chapter 2 presents a Literature Review, giving an overview and timeline of the research subject and different approaches taken in the past. It also explains how this research is a step ahead and makes it of great importance in a WC system.

Chapter 3 starts with an overview of space-time codes (STC) techniques. Then a detailed review of the Alamouti's STBC technique is introduced for ideal WC systems, with

emphasis on the two-transmit one receive diversity STBC scheme. This scheme is further presented with their performance analysis under unknown CSI and imperfect estimates of these channel coefficients, as proposed by Tarokh. Discussing the impairments due to CFO, this STBC system model is further extended incorporating the error variances of the erroneous estimates of CFO into the system.

Chapter 4 a detailed review of the three of the most prevalent detection techniques is introduced with their performance analysis for ideal WC systems. The three detection techniques are

- Maximum Likelihood (ML) detector
- Maximal Ratio Combiner (MRC) with ML detector
- Minimum Mean Square Error detector (MMSE)

Chapter 4 also emphasizes on the effect of these detection techniques in a practical WC systems with CSI and CFO estimation errors.

The proposed detection algorithms are derived in Chapter 5 for all the three different techniques and the generalized form for these algorithms are also presented. This chapter also provides the mathematical calculations how the proposed detectors converges to the conventional detection algorithms. Chapter 5 also shows the BER performance of the proposed algorithms for different modulation schemes in comparison to the conventional detectors. Experimental results are also shown for different estimation error variances.

Chapter 6 summarizes the research along with related ideas for future work. All relevant mathematical calculations required for proper understanding of the thesis is presented in Appendix A.

Chapter 2

Literature Review

The advent of 3G Long Term Evolution (LTE) deployed MIMO smart antenna technology in their system. Although the MA technology is not a recent one, its foundation was laid by Winters in 1984 [41] and Salz in 1985 [42]. Considerable research was done to exploit its benefits [21–23]. However, after Telatar [35], Foschini [43] and Gans [44] recognized its enormous capacity gain, MIMO became a powerful tool for substantial data rates in an extreme fading environment. MA transmit diversity is employed in downlink of a wireless system to enhance the capacity and expand the coverage of the broadcasted signal [45–48]. On the other hand, MA at the receiver is capable of dealing with multipath fading [32]. To cater the increasing demands of higher data throughput and lower latency without any increase in bandwidth, the concern was of more sophisticated technology. Thus, MIMO became an area of interest for researchers [33, 36].

The evolution of 4G LTE radio access wireless technology promised significant improvements in the system performance. LTE Advanced is capable to support MA with both beam forming and spatial multiplexing as proposed by Naguib, Paulraj and Kailath in 1993 [49]. Besides LTE, MIMO is also in wide use in high data rate technologies like IEEE 802.11n (Wifi), WiMAX and HSPA+.

MIMO deploys multiple antennas between the transmitter and the receiver that uses multipath for propagation. However, the signal undergoes severe random fades in a multiple channel transmission, introducing co channel interference and even loss of data as explained in Chapter 1. Thus, the challenge was to design an algorithm, which is efficient enough to render improved spectral efficiency, quality and reliable transmission of the baseband signal under the fading environment. The advanced wireless communication (WC) system exploited STC, which provides space, time and code diversity to combat fading in the MIMO system [50]. Space diversity provided by MIMO is preferred over time and frequency diversity because it does not incur extra time and bandwidth for higher data propagation [34].

Tarokh et al. [51] proposed space-time trellis coding (STTC) in 1998. He used Trellis representation, invented by Gottfried Ungerboeck in 1987 [52], to exploit its property of high efficiency transmission over band-limited channels. However, the coding procedure involved several iterations, which increased its computation and time complexity. Alamouti in 1998, offered a remarkable STBC scheme [29] which provided high diversity gain in MIMO system and proved to have less decoding complexity than Tarokh's STTC. Alamouti used transmit diversity with 2 antennas at the base station (BS) which he further extended to multiple transmit antennas. His novel contribution became a benchmark in the field of WC which opened doors for researchers like Jafarkhani, Scaglione, Hassibi to develop some more significant STC algorithms [53–56].

Tarokh emphasized the effect of a practical multi fading channel and introduced the consequences of the uncertainties. He explored the avenue of channel estimation error while detection and proposed a new decision metric for ML decoding [57]. It is proposed for STTC, however, it is prevalently used as a generalized detection metric for all MIMO systems [58]. Besides accurate estimation and correction of CSI, another challenge to achieve an optimal detection of the data signal is to synchronize transmitter and receiver.

In the practical scenario, CFO occurs unavoidably in an unsynchronized system or even due to oscillator's impairments which perturb the system synchronization. This carrier frequency mismatch disrupts the orthogonality between the carriers introducing ICI. The attempt to improve the system performance has always been made by extensive research on enhancing the accuracy of CFO estimator [59,60], however, few work has been done on detector design by incorporating CFO as a deterministic value [61,62]. The work presented in this thesis emphasizes the effect of estimation error on unsynchronized systems and aims to derive new decoding algorithms under the mismatch scenario.

Chapter 3

Space-Time Block Coding

3.1 Introduction

With the advent of smart antenna technology, Diversity schemes evolved remarkably to help mitigate fading in a highly scattering multipath channel, as discussed in Chapter 1. In the same era STC technique were evolved when the potential of Space, Time and Code diversity was exploited, Fig. 3.1. STC technique is employed to transmit multiple copies of the encoded baseband signal over multiple antennas. This technique improved the throughput and reliability of data transmission over multiple paths.

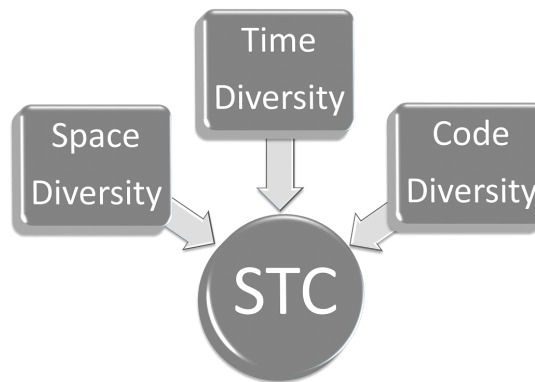


Figure 3.1: Space Time Coding.

As mentioned in Chapter 2, Tarokh proposed STTC [51] in 1998. STTC uses trellis coding for encoding the baseband signal. STTC technique explores space, time and code diversity and thus enlarges the scope of MIMO antenna technology. However, STTC requires Viterbi algorithm at the receiver, which increases its decoding complexity and hence make it improper for practical implementations.

In 1998 Alamouti invented the simplest STBC scheme [29] for MIMO system, which proved to be less complex and more efficient than any STC algorithm [63]. Alamouti harnessed the spatial diversity of transmit antennas to keep the receiver small, compact and less complex. His code diversity promises to maintain orthogonality between the multiple carriers and uses a simple ML decoding algorithm at the receiver.

In this chapter we will provide the system model and brief description on Alamouti's STBC technique. Next we will review the practical scenario when CSI is unknown to the receiver, as proposed by Tarokh. Furthermore, we will propose and derive the system model taking into account the unsynchronized system adding unavoidable CFO into the signal. Then we will derive the system model taking into consideration imperfect estimates of the channel state parameters and the CFO at the receiver. Finally, we will examine the behavior of the BER over SRN curves of STBC system models accounting various assumptions of unknown CSI and CFO.

3.2 STBC System Model

Alamouti's two branch transmit diversity STBC scheme was based upon three functions which will be discussed in details.

- **Transmitter:** Encoding of the baseband signal and its transmission sequence
- **Receiver:** A maximal ratio combiner for multiple transmitted signals
- **Detector:** A maximum likelihood detector for optimal detection of the baseband signal

3.2.1 STBC Transmitter

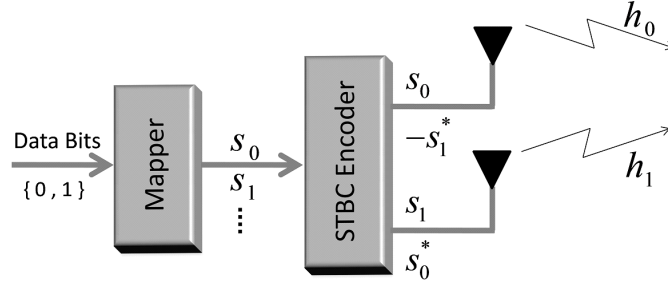


Figure 3.2: Space Time Block Coding transmitter.

Fig. 3.2 demonstrates Alamouti's two-transmit one receive antenna STBC system model which basically comprises of a mapper and an encoder. In Alamouti's STBC scheme is applied to the complex baseband symbols generated by the mapper at the transmitter end. The baseband or data symbols are assumed to be iid with unit variance and the mapped signals can be M-PSK or M-QAM modulated. The symbols are encoded in space and time in such a way that they form orthogonality between the two transmitting antennas. As shown in Table. 3.1, during first time period , symbol s_0 is transmitted from antenna 0 and symbol s_1 is transmitted from antenna 1 simultaneously. In the next symbol duration $t + T$, $-s_1^*$ is transmitted from antenna 0 and symbol s_0^* is transmitted from antenna 1, where $[\cdot]^*$ is the complex conjugate operator.

Table 3.1: Data transmission

Time	Antenna 0	Antenna 1
t	s_0	s_1
$t+T$	$-s_1^*$	s_0^*

The baseband signal is then mounted on a high frequency carrier signal and transmitted

over the wireless channel. The channel $h_i \sim \mathcal{N}(0, 1)$ is modeled as a flat Rayleigh fading channel between the i^{th} transmit antenna and the receive antenna where the channel parameters are complex Gaussian random variables. The channel parameters are assumed flat and are modeled as

$$\begin{aligned} h_0(t) &= h_0(t + T) = h_0 = \alpha_0 e^{j\alpha_0} \\ h_1(t) &= h_1(t + T) = h_1 = \alpha_1 e^{j\alpha_1} \end{aligned} \quad (3.1)$$

which mean the channel is constant for two period of frame of symbols.

3.2.2 STBC Receiver

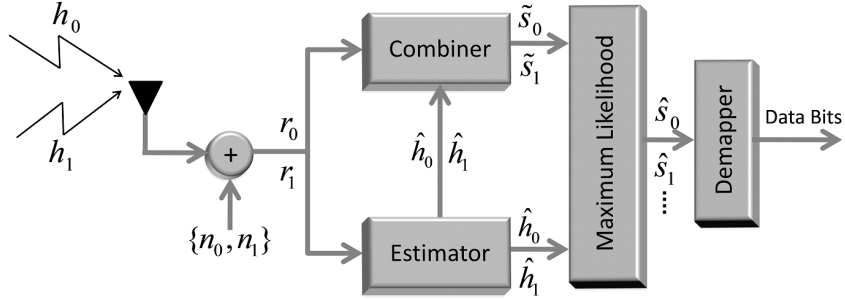


Figure 3.3: Space Time Block Coding receiver.

With a two transmit one receive antenna STBC system, the received signal at two time instants, effected by external noise is modeled as

$$\begin{aligned} r(t) &= h_0 s_0 + h_1 s_1 + n(t) \\ r(t + T) &= -h_0 s_1^* + h_1 s_0^* + n(t + T) \end{aligned} \quad (3.2)$$

where $n(t) \sim \mathcal{N}(0, 2\sigma_n^2)$ is the additive white Gaussian noise (AWGN) with zero mean and variance σ_n^2 per dimension. The STBC receiver block diagram is demonstrated in Fig. 3.3, which describes the baseband signal after demodulation and sampling. Thus, the received signal $r(t)$ when demodulated and sampled at k^{th} instant, we get the baseband signal which

can be expressed as

$$r_k = \sum_{i=0}^{m-1} h_i s_{i,k} \sqrt{E_s} + n_k \quad (3.3)$$

where $\sqrt{E_s}$ is the symbol energy and m are the total number of transmit antennas. Thus the two transmit one receive antenna system can be modeled in a matrix form as

$$\underbrace{\begin{bmatrix} r_0 \\ r_1^* \end{bmatrix}}_R = \underbrace{\begin{bmatrix} h_0 & h_1 \\ h_1^* & -h_0^* \end{bmatrix}}_H \underbrace{\begin{bmatrix} s_0 \\ s_1 \end{bmatrix}}_S + \underbrace{\begin{bmatrix} n_0 \\ n_1^* \end{bmatrix}}_N. \quad (3.4)$$

3.2.2.1 MRC combiner scheme

This combining scheme is said to provide optimal solution in terms of SNR [24]. All the signals from the antenna array are combined in a way that the resulting signal has the maximum SNR. The MRC scheme is discussed in detail in Chapter 4.

Alamouti assumed a perfect estimator of the channel parameters at the receiver, such that $\hat{h}_i = h_i$. Thus, the MRC combiner, combiner the multiple received signals to retrieve the baseband signal s_0 and s_1 in the following way,

$$\begin{aligned} \underbrace{\begin{bmatrix} \tilde{s}_0 \\ \tilde{s}_1 \end{bmatrix}}_{\tilde{S}} &= \underbrace{\begin{bmatrix} h_0 & h_1 \\ h_1^* & -h_0^* \end{bmatrix}}_{H^H} \underbrace{\begin{bmatrix} r_0 \\ r_1^* \end{bmatrix}}_R \\ &= \underbrace{\begin{bmatrix} h_0^* r_0 + h_1 r_1^* \\ h_1^* r_0 - h_0 r_1^* \end{bmatrix}}_{H^H R} \end{aligned} \quad (3.5)$$

where \tilde{s}_0, \tilde{s}_1 are the optimal solution of the MRC in terms of maximum SNR and $[.]^H$ is the

Hermitian operator. Substituting r_k from (3.4) in (3.5)

$$\begin{aligned}\tilde{s}_0 &= (\alpha_0^2 + \alpha_1^2) s_0 + h_0^* n_0 + h_1 n_1^* \\ \tilde{s}_1 &= (\alpha_0^2 + \alpha_1^2) s_1 - h_0 n_1^* + h_1^* n_0\end{aligned}\tag{3.6}$$

The MRC estimates are fed to the ML detector where a hard decision is made between the estimated outputs and the expected codeword as explained next.

3.2.2.2 ML decision scheme

The hard decision criteria used in the ML detector is the Squared Euclidean distance (SED). The SED between x and y is defined as $d^2(x, y) = (x - y)(x^* - y^*)$. The ML decision rule at the receiver is to choose \hat{s}_i and \hat{s}_j , the maximum likelihood of the two transmitted symbols s_0 and s_1 , from a known set of codewords, which can make the following expression minimum

$$\begin{aligned}d^2(r_0, \{h_0 \hat{s}_i + h_1 \hat{s}_j\}) + d^2(r_1, \{-h_0 \hat{s}_j^* + h_1 \hat{s}_i^*\}) \\ \leq d^2(r_0, \{h_0 \hat{s}_k + h_1 \hat{s}_l\}) + d^2(r_1, \{-h_0 \hat{s}_l^* + h_1 \hat{s}_k^*\})\end{aligned}\tag{3.7}$$

for all possible combinations of i, j and k, l such that $\{i, j\} \neq \{k, l\}$. The expression in (3.7) reduces to

$$\begin{aligned}(\alpha_0^2 + \alpha_1^2)|\hat{s}_i|^2 - \hat{s}_i^* \tilde{s}_0 - \hat{s}_i \tilde{s}_0^* \leq (\alpha_0^2 + \alpha_1^2)|\hat{s}_k|^2 - \hat{s}_k^* \tilde{s}_0 - \hat{s}_k \tilde{s}_0^* \quad \forall i \neq k. \\ (\alpha_0^2 + \alpha_1^2)|\hat{s}_j|^2 - \hat{s}_j^* \tilde{s}_1 - \hat{s}_j \tilde{s}_1^* \leq (\alpha_0^2 + \alpha_1^2)|\hat{s}_l|^2 - \hat{s}_l^* \tilde{s}_1 - \hat{s}_l \tilde{s}_1^* \quad \forall j \neq l.\end{aligned}\tag{3.8}$$

for individual ML decision for s_0 and s_1 , which can be generalized for all modulation schemes as follows

$$\begin{aligned}(\alpha_0^2 + \alpha_1^2 - 1)|\hat{s}_i|^2 + d^2(\hat{s}_i, \tilde{s}_0) \leq (\alpha_0^2 + \alpha_1^2 - 1)|\hat{s}_k|^2 + d^2(\hat{s}_k, \tilde{s}_0) \quad \forall i \neq k. \\ (\alpha_0^2 + \alpha_1^2 - 1)|\hat{s}_j|^2 + d^2(\hat{s}_j, \tilde{s}_1) \leq (\alpha_0^2 + \alpha_1^2 - 1)|\hat{s}_l|^2 + d^2(\hat{s}_l, \tilde{s}_1) \quad \forall j \neq l.\end{aligned}\tag{3.9}$$

However, PSK being a special case with equal energy constellations $|s_i|^2 = E_s$ for all values of i, j, k, l , the ML decision scheme can be reduced to

$$\begin{aligned}d^2(\hat{s}_i, \tilde{s}_0) \leq d^2(\hat{s}_k, \tilde{s}_0) \quad \forall i \neq k. \\ d^2(\hat{s}_j, \tilde{s}_1) \leq d^2(\hat{s}_l, \tilde{s}_1) \quad \forall j \neq l.\end{aligned}\tag{3.10}$$

Alamouti's assumption of a perfect estimation is impractical in real scenarios. The researchers are doing a lot of pioneering work to achieve an ideal estimator, however, there still exists some minute errors in its estimation. Tarokh assumed a practical non-ideal estimator and introduced the erroneous values in the detection techniques to optimize the output to a more precise value. In the following section we will incorporate the erroneous estimates of a practical non-ideal estimator to our system.

3.3 Effect of parameter estimation errors

This section will focus on the effect of different parameter estimation errors on the system model mentioned above, where all derivations were done assuming that the receiver has a perfect estimation of the channel parameters and is perfectly tuned to the CFO. In subsection 3.3.1, the effects of channel estimation error is discussed for the STBC system as proposed by Tarokh. Subsection 3.3.2 performs a similar analysis with the effect of CFO estimation errors. At the end of each section demonstrates how the performance of the ideal system degrades when the estimator gives erroneous estimation of both the parameters.

3.3.1 System model with unknown CSI

Vahid Tarokh proposed a decision matrices for a STBC system where receiver has no knowledge of the CSI. He assumes the output of the channel estimator to be erroneous and modeled it as

$$\hat{h}_i = h_i + \varepsilon_i, \quad (3.11)$$

where \hat{h}_i is the imperfect channel estimate and ε_i is the estimation error independent of h_i .

Tarokh demonstrated the proof using orthogonal pilot sequence insertion (O-PSI) method to insert pilot symbols at the beginning of each frame of data symbols, which is known to the receiver and help in estimating the channel parameters. Here, the baseband signal in (3.3) during the training, can be modified to show the relationship between the received

signal and the pilots as

$$r_l = \sum_{i=0}^{m-1} h_i p_{i,l} + n_l \quad (3.12)$$

where $P = [p_{i,1} \ p_{i,2} \ \dots \ p_{i,l}]$ is the set of transmitted pilot symbols of length l from i^{th} antenna and $r_l = [r_1 \ r_2 \ \dots \ r_l]$ is the set of received observation over the length l . The MMSE estimate of the channel fading parameters can be obtained as

$$\begin{aligned} \hat{h}_i &= \frac{r_l P^H}{P P^H} \\ &= \frac{r_l P^H}{\|P\|^2}. \end{aligned} \quad (3.13)$$

Designing the pilot symbols as orthogonal to each other, we can easily write (3.12) as

$$\begin{aligned} r_l P^H &= h_i \|P\|^2 + n_l P^H \\ \Rightarrow h_i &= \frac{r_l P^H}{\|P\|^2} - \frac{n_l P^H}{\|P\|^2} \\ \Rightarrow \hat{h}_i &= h_i + \underbrace{\frac{n_l P^H}{\|P\|^2}}_{\varepsilon_i}. \end{aligned} \quad (3.14)$$

The channel estimation error $\varepsilon_i \sim \mathcal{N}(0, \sigma_\varepsilon^2)$ is considered a zero mean Gaussian random variable (RV) with variance σ_ε^2 and is assumed to be a function of signal-to-noise ratio, number of pilot symbols and the method of estimation. Using the relation in (3.11), it can be easily concluded that the imperfect estimate $\hat{h}_i \sim \mathcal{N}(0, \sigma_{\hat{h}}^2)$ is also a Gaussian RV with mean zero and variance $\sigma_{\hat{h}}^2$.

Thus the system model in (3.5) modifies to

$$\underbrace{\begin{bmatrix} \tilde{s}_0 \\ \tilde{s}_1 \end{bmatrix}}_{\tilde{\mathbf{S}}} = \underbrace{\begin{bmatrix} \hat{h}_0^* r_0 + \hat{h}_1 r_1^* \\ \hat{h}_1^* r_0 - \hat{h}_0 r_1^* \end{bmatrix}}_{\hat{H}^H R} \quad (3.15)$$

$$= \underbrace{\begin{bmatrix} h_0^* r_0 + h_1 r_1^* + \varepsilon_0^* r_0 + \varepsilon_1 r_1^* \\ h_1^* r_0 - h_0 r_1^* + \varepsilon_1^* r_0 - \varepsilon_0 r_1^* \end{bmatrix}}_{(H+\varepsilon)^H R}$$

Therefore, an imperfect estimator leaves behind some estimation errors in the detection of the baseband signal. The demerits of ignoring the estimation error is shown in the performance graph at the end of the chapter, where the signal deteriorates in comparison to the detection with perfect estimate.

3.3.1.1 Simulation performance of unknown CSI

In this section the performance of a two transmit one receive STBC system is analyzed in the presence of CSI estimation errors. Fig. 3.4 demonstrates the performance of 4-PSK modulated STBC system with unknown flat Rayleigh fading channel. The graph shows how the length of pilot symbols effect the estimation of the unknown channel at the receiver as given by Cramer-Rao bound. The minimum value of the estimation error variance is

$$\sigma_\varepsilon^2 = \frac{N_0}{lE_s}, \quad (3.16)$$

where l is the length of pilot symbols transmitted during training. The simulation is performed by transmitting 10^4 frames of data symbols with a frame length of 130 symbols. The results are analyzed by plotting the BER against multiple values of SNR

Fig. 3.5 demonstrates the performance of 8-PSK and 16-PSK modulated STBC system with unknown channel parameters. The performance is shown to degrade with increasing modulation scheme.

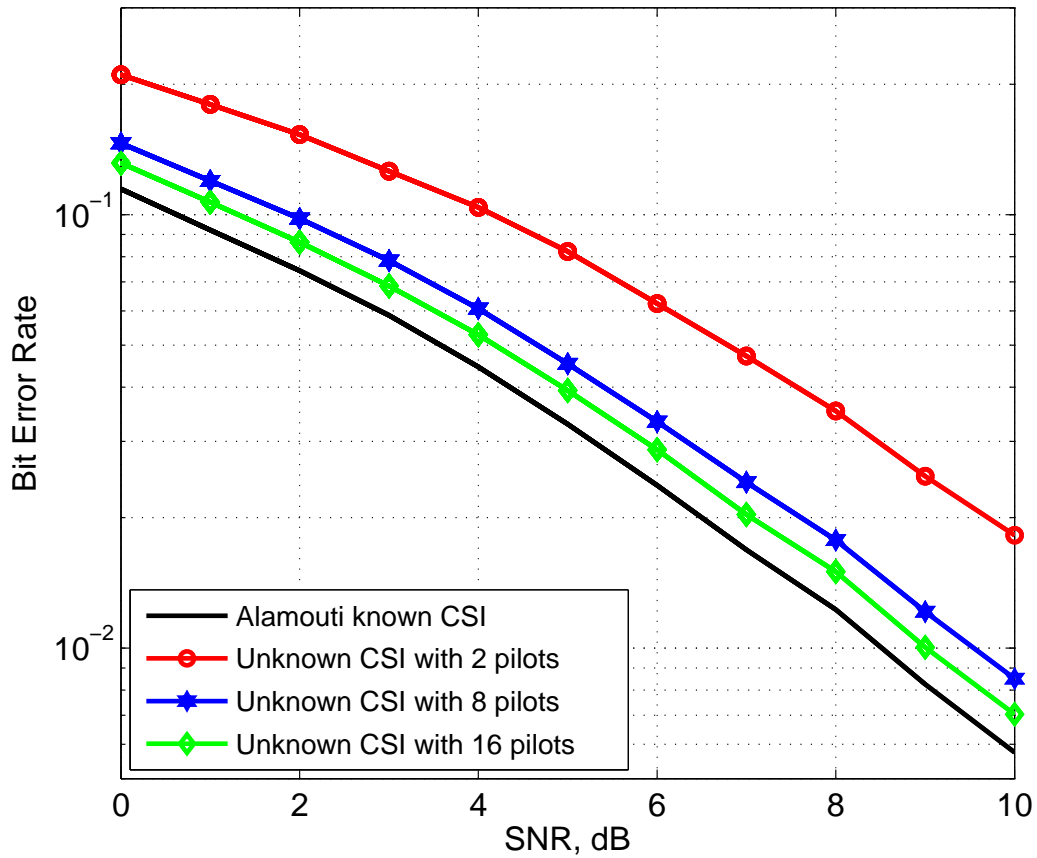
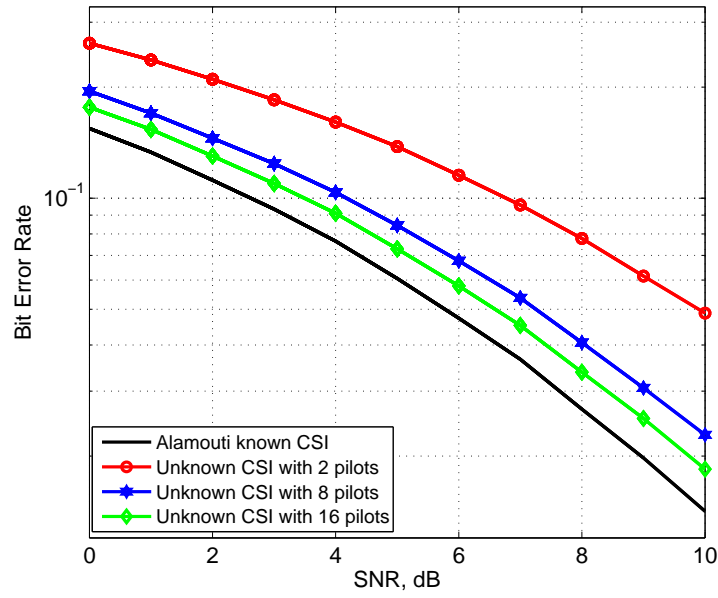
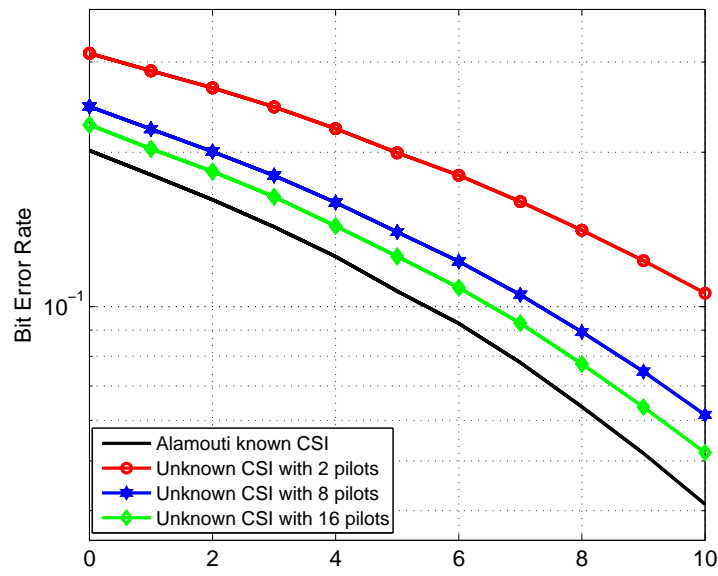


Figure 3.4: Performance of 4-PSK STBC system for different pilot length.

Fig. 3.6 demonstrates the performance of 4-QAM and 16-QAM modulated STBC system with unknown channel parameters. QAM modulation is considered for the case of non equal energy constellations. It is known from standard literature that, the performance of higher amplitude modulation scheme is susceptible to high BER and it increases under the mismatch scenario.

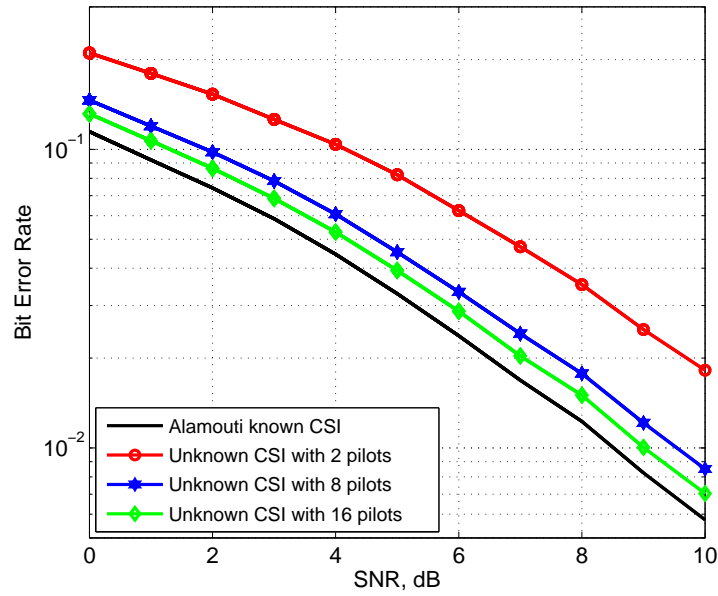


(a) 8-PSK

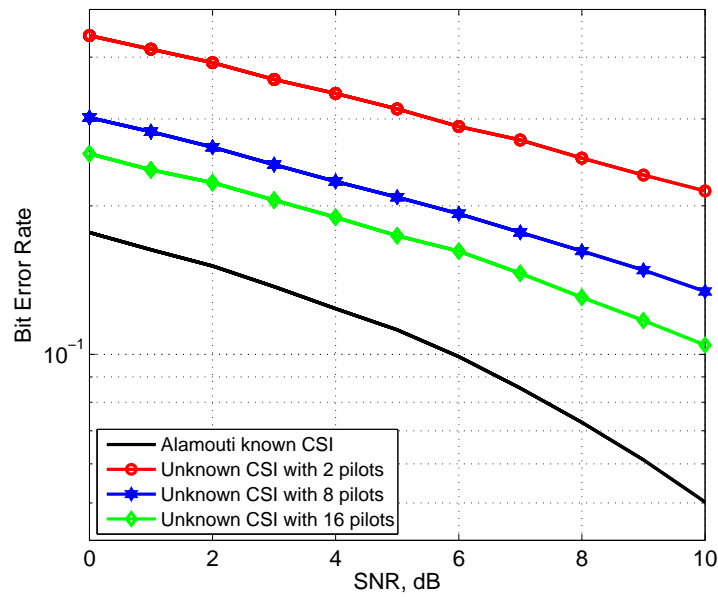


(b) 16-PSK

Figure 3.5: Performance of M-PSK STBC system for different pilot length.



(a) 4-QAM



(b) 16-QAM

Figure 3.6: Performance of M-QAM STBC system for different pilot length.

3.3.2 System model with unknown CFO

It is discussed in section 1.3.2, that in practical systems the receiver oscillator frequency and the transmitter's carrier frequency mismatches or is not perfectly synchronized. This mismatch is known as CFO $\Delta f_{i,k}$ which varies with different channels between i^{th} transmit and receive antenna and with different sampling times k , as shown in Table 3.2

Table 3.2: CFO distribution with channel and time

Time	Channel 0	Channel 1
$t=0$	Δf_{00}	Δf_{10}
$t+T$	Δf_{01}	Δf_{11}

Thus, the received baseband signal with CFO can be modeled as

$$r_k = \sum_{i=0}^{m-1} h_i e^{j\phi_{i,k}} s_{i,k} \sqrt{E_s} + n_k \quad (3.17)$$

where $\phi_{i,k} = 2\pi \Delta f_{i,k} / f_s$ is the carrier angular frequency offset (CAFO) which is assumed to be a Gaussian RV with zero mean and variance σ_ϕ^2 and f_s is the sampling frequency, similar to the assumptions made in [64,65]. This representation is vastly used in literature [66] and is only valid when assumed $\Delta f_{i,k} \ll f_s$. Thus for a two branch STBC system, CAFO can be represented in a matrix form as

$$\Phi_{i,k} = \begin{bmatrix} \phi_{00} & \phi_{10} \\ \phi_{01} & \phi_{11} \end{bmatrix} \quad (3.18)$$

In reality, the CAFO is unknown to the receiver and is estimated before detection. Irrespective of the type of estimator, the CAFO estimate $\hat{\phi}_{i,k}$ is modeled same as that of the channel estimate in (3.11).

$$\hat{\phi}_{i,k} = \phi_{i,k} + \epsilon_{i,k} \quad (3.19)$$

The estimation error $\epsilon_{i,k} \sim \mathcal{N}(0, \sigma_\epsilon^2)$ is considered a zero mean Gaussian RV. Since, the original value of CAFO $\phi_{i,k}$ and the estimation error $\epsilon_{i,k}$ are independent of each other, the imperfect estimate is also a Gaussian RV $\hat{\phi}_{i,k} \sim \mathcal{N}(0, \sigma_{\hat{\phi}}^2)$.

To simplify the system model, let us substitute $x_{i,k}$ for $h_i e^{j\phi_{i,k}}$. Therefore matrix X can be expressed as

$$X = \begin{bmatrix} x_{00} & x_{10} \\ x_{11}^* & -x_{01}^* \end{bmatrix} = \begin{bmatrix} h_0 e^{j\phi_{00}} & h_1 e^{j\phi_{10}} \\ (h_1 e^{j\phi_{11}})^* & -(h_0 e^{j\phi_{01}})^* \end{bmatrix}. \quad (3.20)$$

Thus the system model in (3.15) modifies to

$$\underbrace{\begin{bmatrix} \tilde{s}_0 \\ \tilde{s}_1 \end{bmatrix}}_{\tilde{\mathbf{s}}} = \underbrace{\begin{bmatrix} \hat{x}_{00}^* r_0 + \hat{x}_{10} r_1^* \\ \hat{x}_{11}^* r_0 - \hat{x}_{01} r_1^* \end{bmatrix}}_{\hat{X}^H R} \quad (3.21)$$

$$= \begin{bmatrix} \hat{h}_0^* e^{-j\hat{\phi}_{00}} r_0 + \hat{h}_1 e^{j\hat{\phi}_{11}} r_1^* \\ \hat{h}_1^* e^{-j\hat{\phi}_{10}} r_0 - \hat{h}_0 e^{j\hat{\phi}_{01}} r_1^* \end{bmatrix}$$

Therefore, when the estimator is imperfect, it leaves behind estimation errors in the detection of the baseband signal. The simulation demonstrates the deterioration of the baseband signal effected by CFO and CSI estimation errors as comparison to the ideal system.

3.3.2.1 Simulation performance of unknown CFO

Fig. 3.7 demonstrates the performance of 4-PSK modulated STBC system for an unsynchronized unknown carrier frequency offset and CSI.

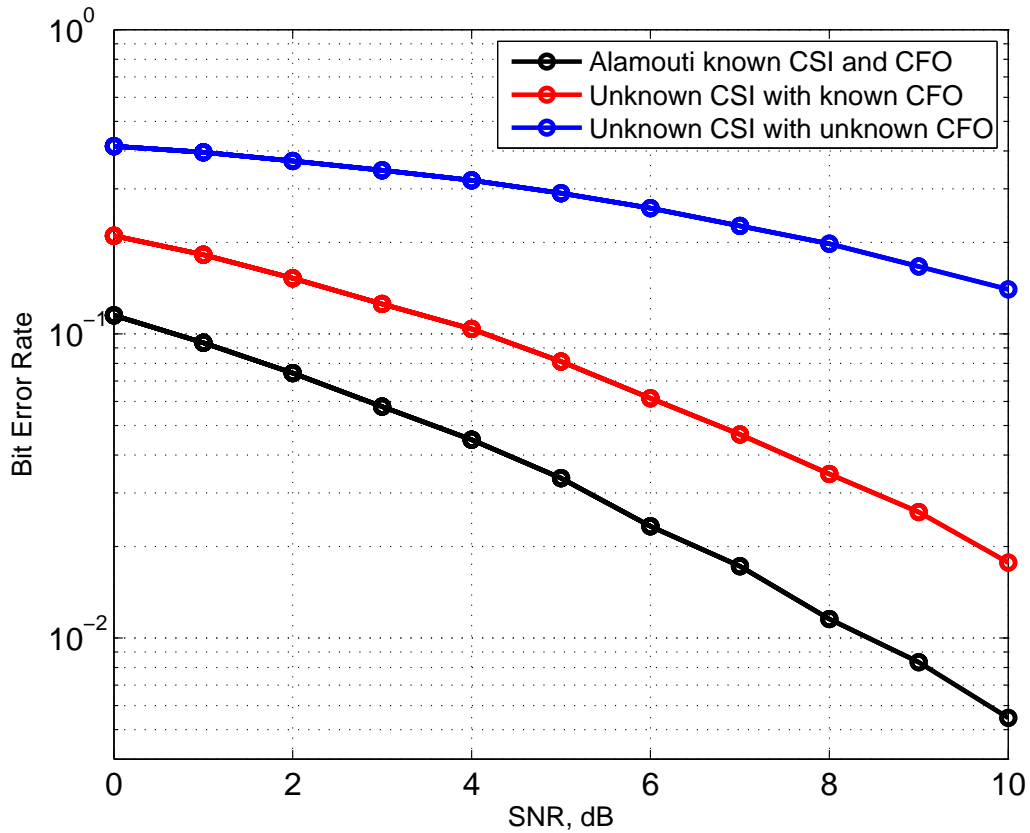
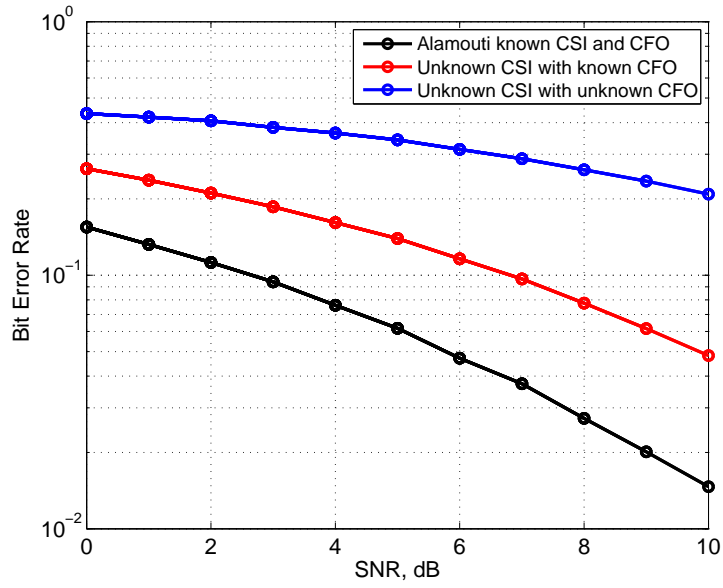
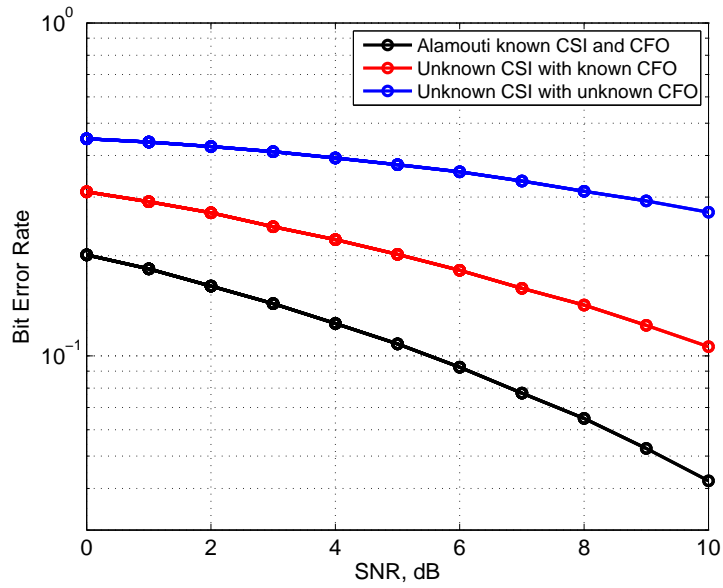


Figure 3.7: Performance of unsynchronized 4-PSK STBC system under mismatch scenario.

Fig. 3.8 demonstrates the performance of 8-PSK and 16-PSK modulated unsynchronized STBC system. The performance is shown to degrade with increasing modulation scheme. The graphs shows how the system BER deteriorates when CSI is unknown and it gets worst when the system is unsynchronized, adding CFO into the system.



(a) 8-PSK



(b) 16-PSK

Figure 3.8: Performance of unsynchronized M-PSK STBC system under mismatch scenario.

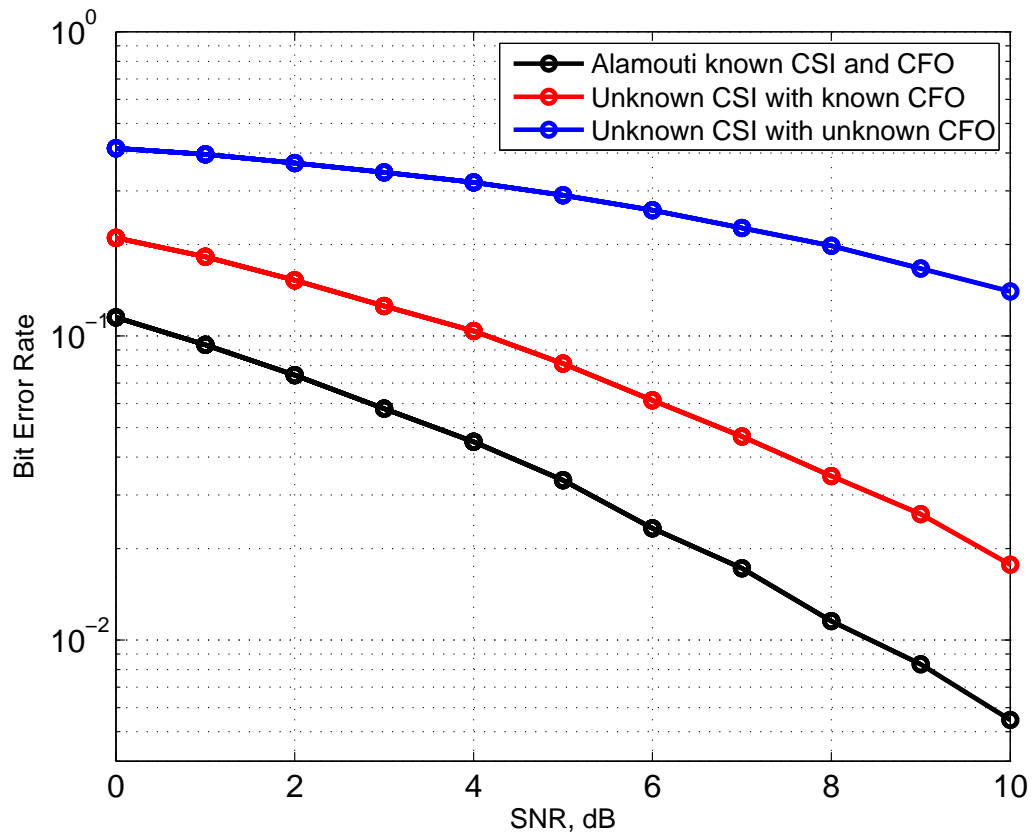
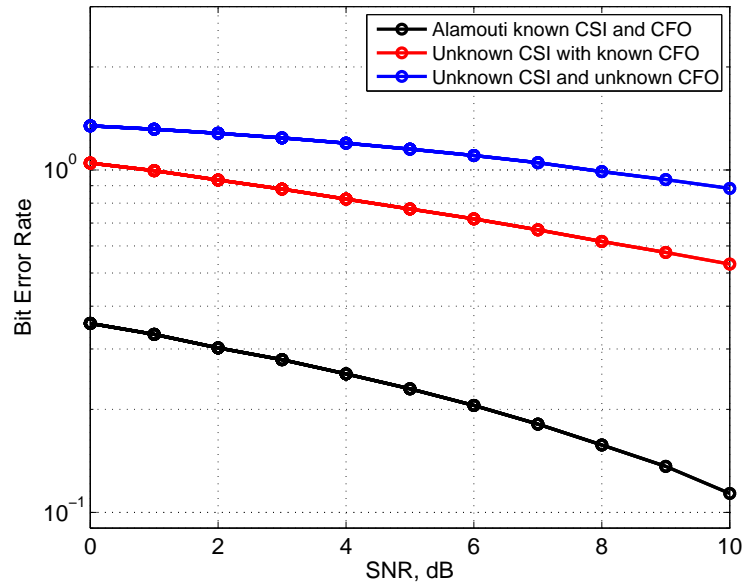
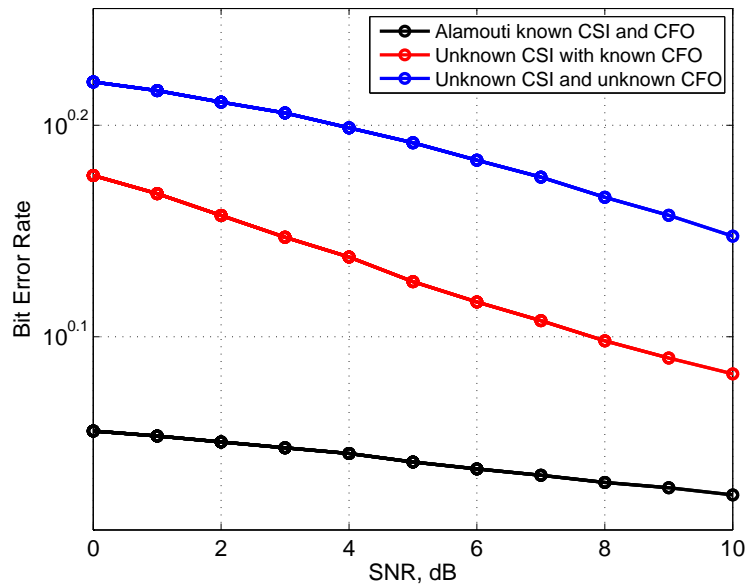


Figure 3.9: Performance of unsynchronized 4-QAM STBC system under mismatch scenario.

Fig. 3.9 is shown for the basic 4-QAM and demonstrates similar performance as that of QPSK. Fig. 3.10 (a) and (b) demonstrates the performance of the STBC system for 16-QAM and 64-QAM respectively. QAM modulation is considered for the case of non equal energy constellations. It is known from standard literature that, the performance of higher amplitude modulation scheme is susceptible to high BER and it increases under the mismatch scenario.



(a) 16-QAM



(b) 64-QAM

Figure 3.10: Performance of unsynchronized M-QAM STBC system under mismatch scenario.

Chapter 4

STBC detection techniques

As a matter of fact, receiver is of utmost importance, because of its incredible task in a WC system. It receive a signal for a fraction of time, observe and retrieve the baseband signal from it, and make the best estimate of the transmitted signal. In the presence of multiplicative unknown channel coefficients and additive noise, the detection technique at the receiver takes account of this decision making process and once in a while make occasional errors. Thus, a best detector is the one, which is optimal in the sense of minimizing the BER.

This chapter focuses on the detection schemes most prominently used at the receiver for an optimal detection of the baseband signal. The subsections take into account the unknown channel parameters and the CFO and follows the certainty equivalence principle (CEP) for the purpose of design. The CEP states that the estimates of the uncertainties are treated as if they were the true parameters and hence are used to derive the conventional detection schemes. With this approach, we determine, that the conventional schemes give a poor performance with CEP as compared to the proposed schemes.

4.1 Maximum Likelihood detector

Maximum Likelihood is a detection method based on a set of observations for a given statistic by maximizing the likelihood function. Considering the system model presented in (3.3), the received signal r_k at the k -th instant and the channel fading parameters h_i from the i -th transmit antenna are taken as the observations, as shown in Fig. (4.1), whereas the parameter to be detected is the transmitted signal $s_{i,k}$.

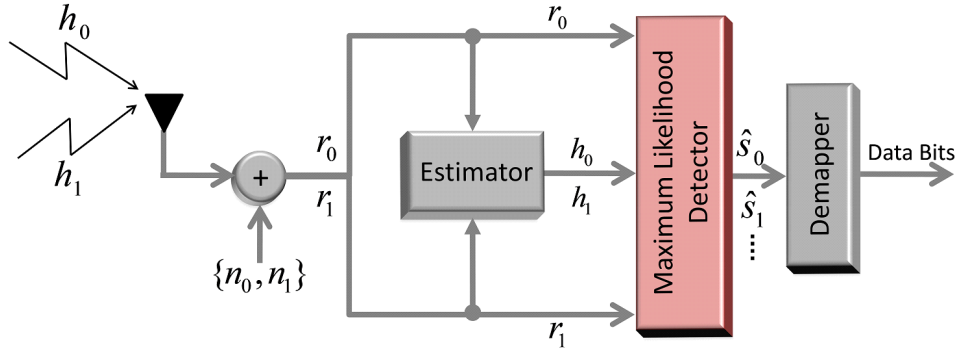


Figure 4.1: Generic block diagram of a ideal ML detector with perfect estimation of channel parameters and no CFO.

4.1.1 ML System discription

The aim of a ML detector is to obtain the optimum value of $\hat{s}_{i,k} = s_{i,k}$ such that the posterior probability of the transmitted signal conditioned on the observations is highest. Optimal detection is obtained by choosing from a finite set of symbols $\mathcal{C} = \{c_0, c_1, \dots\}$, depending upon the type of modulation scheme used at the transmitter. This can be expressed as

$$s_{i,k} \triangleq \arg \max_{s \in \mathcal{C}} \{P(s_{i,k} | r_k, h_i)\}. \quad (4.1)$$

The expression is known as *maximum a posteriori* (MAP) probability function. Using Bayes' theorem [40], (4.1) can be written in the form

$$s_{i,k} \triangleq \arg \max_{s \in \mathcal{C}} \left\{ \frac{P(s_{i,k}) P(r_k | s_{i,k}, h_i)}{(r_k)} \right\}, \quad (4.2)$$

where the probability of receiving r_k conditioned on h_i and when $s_{i,k}$ is transmitted, $P(r_k | s_{i,k}, h_i)$ is known as the *likelihood* function. Since we choose the value of $s \in \mathcal{C}$, $P(s)$ is a constant and hence it can be seen from (4.2), that maximizing the likelihood function maximizes the MAP probability. Thus the decision rule for optimal detection becomes

$$s_{i,k} \triangleq \arg \max_{s \in \mathcal{C}} \{P(r_k | s_{i,k}, h_i)\}. \quad (4.3)$$

The probability distribution of the received signal r_k can be approximated to be of a Gaussian RV as explained in [67]. The PDF of a Gaussian RV is of the form

$$f(r) = \frac{1}{\sqrt{2\pi\sigma_r^2}} e^{\left(\frac{-|r - \mu_r|^2}{2\sigma_r^2}\right)}, \quad (4.4)$$

where μ_r is the mean and σ_r^2 is the variance. By taking the negative logarithm of the likelihood function from (4.4), the decision metric in (4.3) becomes

$$\begin{aligned} s_{i,k} &\triangleq \arg \min_{s \in \mathcal{C}} \{-\log P(r_k | s_{i,k}, h_i)\} \\ &= \arg \min_{s \in \mathcal{C}} \{\|r_k - h_i s_{i,k}\|^2\}. \end{aligned} \quad (4.5)$$

For the Alamouti's STBC two branch MISO system, the ML decision metric for optimal detection of the transmitted signal is

$$s_{i,k} \triangleq \arg \min_{s \in \mathcal{C}} \{|r_0 - h_0 s_0 - h_1 s_1|^2 + |r_1 - h_1 s_0^* + h_0 s_1^*|^2\}. \quad (4.6)$$

ML detection is widely in use for WC systems specially for MIMO. The performance of this detection technique has been studied [68–71] over a period of time, for all types of

MIMO and other wireless systems. This technique has proved to be one of the best in terms of minimizing the BER.

4.1.2 ML detector with unknown CSI based upon CEP

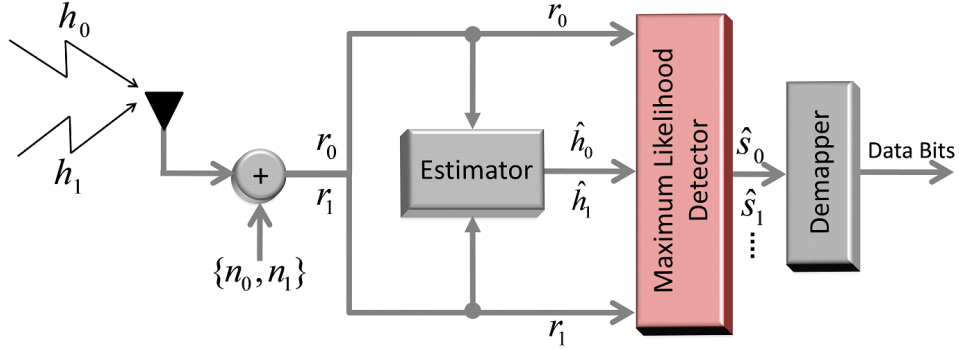


Figure 4.2: Generic block diagram of an ML detector with imperfect estimation of channel parameters and no CFO.

However in the case, when the the estimator at the receiver shown in Fig. (4.2) provides imperfect estimate of the channel parameters \hat{h}_i which is given as an input to the detector. This makes the decision metric

$$s_{i,k} \triangleq \arg \max_{s \in \mathcal{C}} \left\{ P \left(s_{i,k} | r_k, \hat{h}_i \right) \right\}. \quad (4.7)$$

By Bayes' theorem introduced earlier, the decision metric leads to maximizing the likelihood function

$$s_{i,k} \triangleq \arg \max_{s \in \mathcal{C}} \left\{ P \left(r_k | s_{i,k}, \hat{h}_i \right) \right\}. \quad (4.8)$$

Taking negative logarithm and using the relation in (3.11), the ML decision metric is given

in the form

$$\begin{aligned}
s_{i,k} &\triangleq \arg \min_{s \in \mathcal{C}} \left\{ \left| r_0 - \hat{h}_0 s_0 - \hat{h}_1 s_1 \right|^2 + \left| r_1 - \hat{h}_1 s_0^* + \hat{h}_0 s_1^* \right|^2 \right\} \\
&= \arg \min_{s \in \mathcal{C}} \left\{ \left| r_0 - (h_0 + \varepsilon_0) s_0 - (h_1 + \varepsilon_1) s_1 \right|^2 \right. \\
&\quad \left. + \left| r_1 - (h_1 + \varepsilon_1) s_0^* + (h_0 + \varepsilon_0) s_1^* \right|^2 \right\}
\end{aligned} \tag{4.9}$$

This form of ML detection metric involves the channel estimation error ε_i and does not provide optimal detection. The degradation of the system performance will be further analyzed by simulation in Chapter 5, section 5.6.

4.1.3 ML detector with unknown CSI & CFO based upon CEP

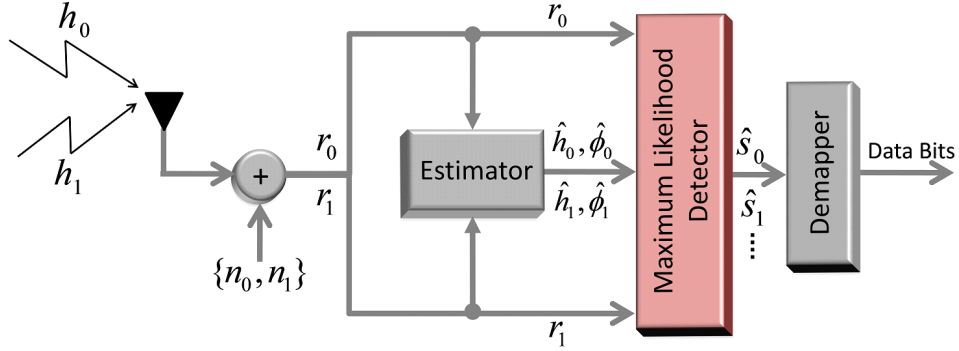


Figure 4.3: Generic block diagram of an unsynchronized ML detector with imperfect estimation of channel parameters.

The ML detector in the presence of channel estimation error maximizes the decision metric given in (4.9). Here we also consider the erroneous estimate of CFO, modeled as (3.17) as shown in Fig. (4.3). This changes the decision metric for choosing $s \in \mathcal{C}$, to

$$s_{i,k} \triangleq \arg \max_{s \in \mathcal{C}} \left\{ P \left(s_{i,k} | r_k, \hat{h}_i, \hat{\phi}_{i,k} \right) \right\}. \tag{4.10}$$

Thus by Bayes' theorem, the likelihood function is

$$s_{i,k} \triangleq \arg \max_{s \in \mathcal{C}} \left\{ P \left(r_k | s_{i,k}, \hat{h}_i, \hat{\phi}_{i,k} \right) \right\}. \quad (4.11)$$

Using the baseband representation in (3.17), the ML detector in the presence of both channel and CFO estimation error becomes

$$\begin{aligned} s_{i,k} &\triangleq \arg \min_{s \in \mathcal{C}} \left\{ \left| r_0 - \hat{h}_0 s_0 e^{j\hat{\phi}_{00}} - \hat{h}_1 s_1 e^{j\hat{\phi}_{10}} \right|^2 + \left| r_1 - \hat{h}_1 s_0^* e^{j\hat{\phi}_{11}} + \hat{h}_0 s_1^* e^{j\hat{\phi}_{01}} \right|^2 \right\} \\ &= \arg \min_{s \in \mathcal{C}} \left\{ \left| r_0 - (h_0 + \varepsilon_0) s_0 e^{j(\phi_{00} + \epsilon_{00})} - (h_1 + \varepsilon_1) s_1 e^{j(\phi_{10} + \epsilon_{10})} \right|^2 \right. \\ &\quad \left. + \left| r_1 - (h_1 + \varepsilon_1) s_0^* e^{j(\phi_{11} + \epsilon_{11})} + (h_0 + \varepsilon_0) s_1^* e^{j(\phi_{01} + \epsilon_{01})} \right|^2 \right\} \end{aligned} \quad (4.12)$$

The presence of estimates \hat{h}_i and $\hat{\phi}_{i,k}$ of CSI and CAFO respectively does not provide optimal detection.

4.2 Maximal Ratio Combiner and ML detection scheme

In the case of two transmit one receive antenna system, the receiver receives two transmitted signals at the same time. Thus, the major challenge in transmit diversity schemes is to effectively detect all the baseband signals received at the same time instant. Transmit diversity combining works by dedicating the signals from the entire array of antennas to form a single signal with the highest SNR. Thus they are more effective when the fading suffered by the multiple copies of the received signal are independent.

The MRC combining scheme is said to provide optimal solution in terms of SNR [24]. All the transmitted signals are combined in a way that the resulting signal has the maximum SNR. The MRC scheme is further discussed in detail in the following section.

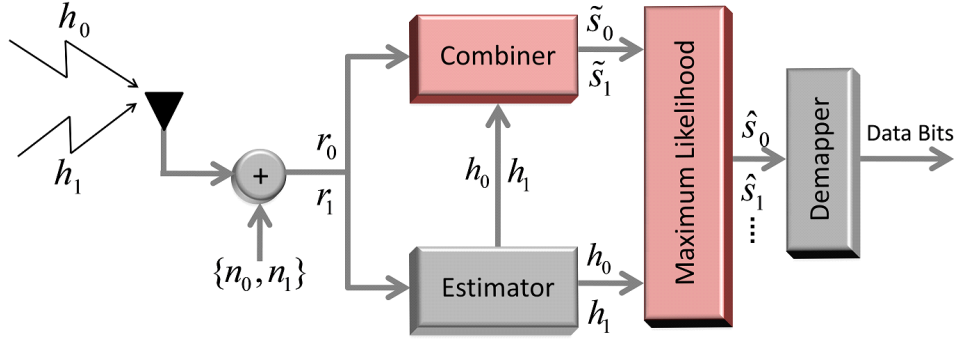


Figure 4.4: Generic block diagram of a ideal MRC detector with perfect estimation of channel parameters and no CFO.

4.2.1 MRC System discription

Fig. (4.4) demonstrates the block diagram of a synchronized receiver with MRC combiner and the ML decision scheme. The general form for a linear combiner is modeled as

$$\tilde{s}_{i,k} = w_0^* r_0 + w_1^* r_1 + \dots + w_{M-1}^* r_{M-1}, \quad (4.13)$$

where w_0 , w_1 and w_{M-1} are the weights for optimal combining of the received signal r_0 , r_1 and r_{M-1} respectively. This system model can be reduced to

$$\tilde{S} = W^H R = W^H (HS + N) \quad (4.14)$$

for a two branch MISO STBC system, where W is a 2×2 combining weight matrix. From (3.4), the above relation can be written as

$$\tilde{S} = W^H (HS + N) \quad (4.15)$$

Assuming that the receiver has perfect knowledge of CSI. The instantaneous SNR can be expressed as

$$SNR = \frac{E [|W^H HS|^2]}{E [|W^H N|^2]} = \frac{\sigma_s^2 |W^H H|^2}{\sigma_n^2 \|W\|^2}. \quad (4.16)$$

Here σ_s^2 and σ_n^2 is the variance of the transmitted signal and the additive noise respectively. Cauchy-Schwarz inequality [72] states the following relation

$$\left| \sum_{i=0}^{M-1} w_i h_i \right|^2 \leq \sum_{i=0}^{M-1} |w_i|^2 \sum_{i=0}^{M-1} |h_i|^2. \quad (4.17)$$

Thus, maximum SNR can be obtained when $W = H$. Substituting this relation in (4.16) we get the maximum value of SNR

$$SNR_{max} = \frac{\sigma_s^2}{\sigma_n^2} \|W\|^2 = \frac{\sigma_s^2}{\sigma_n^2} (|h_0|^2 + |h_1|^2). \quad (4.18)$$

Now, let us substitute the relation $W = H$ in the general form of linear combiners (4.14), to get the expression for MRC

$$\begin{aligned} \tilde{S} &= H^H R \\ &= \begin{bmatrix} h_0 & h_1 \\ h_1^* & -h_0^* \end{bmatrix}^H \begin{bmatrix} r_0 \\ r_1^* \end{bmatrix} \end{aligned} \quad (4.19)$$

which is optimal in the sense of maximizing SNR as derived in (3.5). The ML decision scheme, in conjugation with MRC combiner for a known channel has been explained in section (3.2.2.2).

4.2.2 MRC detector with unknown CSI based upon CEP

However, for a practical case when the channel estimates \hat{H}_i are unknown and are erroneously estimated at the receiver, as given in Fig. (4.5), the MRC scheme in (4.19) becomes

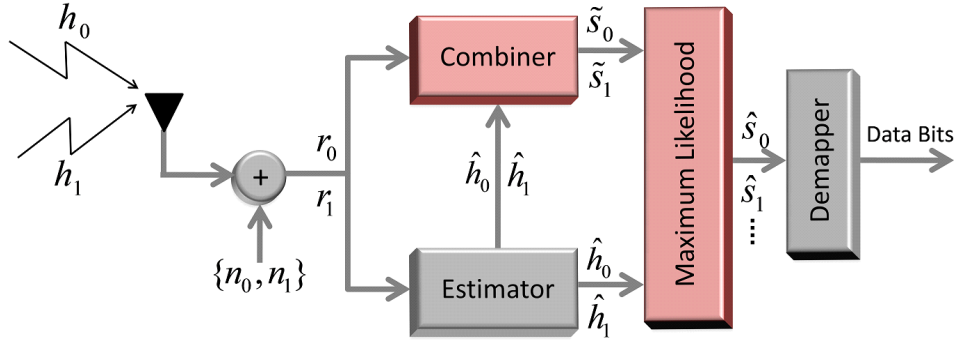


Figure 4.5: Generic block diagram of an MRC detector with imperfect estimation of channel parameters and no CFO.

$$\begin{aligned}
 \tilde{S} &= \hat{H}^H R \\
 &= \begin{bmatrix} \hat{h}_0^* r_0 + \hat{h}_1 r_1^* \\ \hat{h}_1^* r_0 - \hat{h}_0 r_1^* \end{bmatrix}
 \end{aligned} \tag{4.20}$$

which contains erroneous terms (3.15) and thus, does not provide an output with the maximum SNR. Moreover, the ML decision block as in (3.8), with the imperfect channel estimates, decides in favor of

$$\begin{aligned}
 \tilde{s}_{i,k} &\triangleq \arg \min_s \left\{ \left(|\hat{h}_0|^2 + |\hat{h}_1|^2 - 1 \right) |\hat{s}_{i,k}|^2 + d^2 (\hat{s}_{i,k}, \tilde{s}_{i,k}) \right\} \\
 &\Rightarrow \arg \min_s \left\{ (|h_0 + \varepsilon_0|^2 + |h_1 + \varepsilon_1|^2 - 1) |\hat{s}_{i,k}|^2 + d^2 (\hat{s}_{i,k}, \tilde{s}_{i,k}) \right\}.
 \end{aligned} \tag{4.21}$$

With introduction of erroneous estimates, there may occur that $s_{i,k} \neq \tilde{s}_{i,k}$, which will increase BER, aggravating system performance of linear combiner as already shown in the simulations in section (3.3.2.1). In the next section we will study the STBC system model with MRC combiner and ML decision scheme, in the presence of CFO.

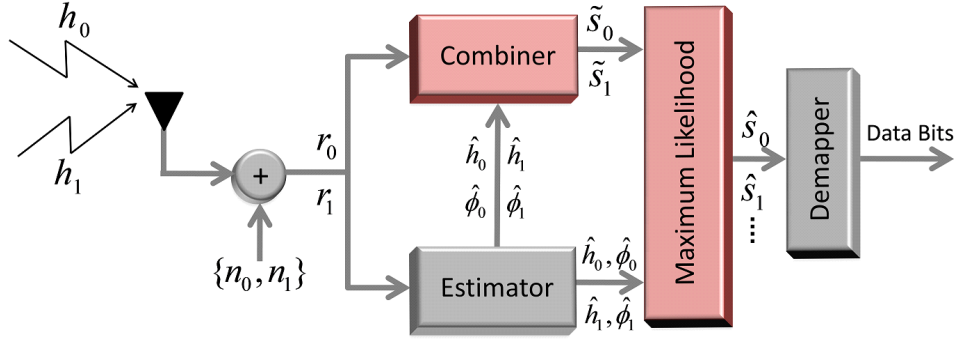


Figure 4.6: Generic block diagram of an unsynchronized MRC detector with imperfect estimation of channel parameters.

4.2.3 MRC detector with unknown CSI & CFO based upon CEP

We have already derived in section (4.2.2) the case when the receiver had perfect knowledge of CFO, however, the estimation of CSI was erroneous. In this section, we will derive the mathematical expression of the MRC combiner, in the presence of both CSI and CFO estimation errors, as shown in Fig. (4.6). The mathematical expression of the combiner as expressed in (4.20) can be modeled as

$$\begin{aligned}
 \tilde{S} &= \hat{X}^H R \\
 &= \begin{bmatrix} \hat{h}_0^* e^{-j\hat{\phi}_{00}} r_0 + \hat{h}_1 e^{j\hat{\phi}_{11}} r_1^* \\ \hat{h}_1^* e^{-j\hat{\phi}_{10}} r_0 - \hat{h}_0 e^{j\hat{\phi}_{01}} r_1^* \end{bmatrix} \\
 &= \begin{bmatrix} (h_0^* + \varepsilon_0^*) e^{-j(\phi_{00} + \epsilon_{00})} r_0 + (h_1 + \varepsilon_1) e^{j(\phi_{11} + \epsilon_{11})} r_1^* \\ (h_1^* + \varepsilon_1^*) e^{-j(\phi_{10} + \epsilon_{10})} r_0 - (h_0 + \varepsilon_0) e^{j(\phi_{01} + \epsilon_{01})} r_1^* \end{bmatrix}
 \end{aligned} \tag{4.22}$$

which has been shown in (3.21). Thus, the presence of CFO estimation error deteriorates the output SNR of the combiner. However, the ML decision scheme given in (4.21) remains the same and has no effect on its performance by the exponential erroneous CFO estimation error.

4.3 Minimum Mean Square Error detector

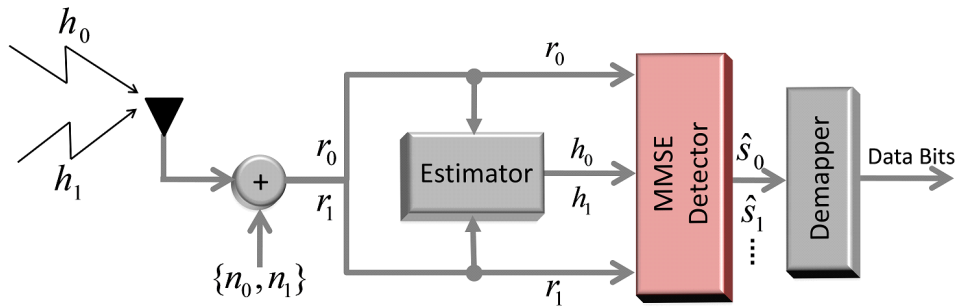


Figure 4.7: Generic block diagram of an ideal MMSE detector with perfect estimation of channel parameters and no CFO.

Fig (4.7) demonstrates block diagram of a linear MMSE detector, which is designed to minimize the squared mean of the error between the original value and the estimated value of the transmitted signal for its optimum detection. In our STBC model, the MMSE detector aims to minimize the mean square error (MSE) between the transmitted signal $s_{i,k}$ and its MMSE estimate $\hat{s}_{i,k}$. Let us consider the case of a two branch MISO system, whose system model can be mathematically expressed in the form

$$R = HS + N, \quad (4.23)$$

already explained in (3.4) The general form of a linear estimator is the following

$$\hat{S} = KR \quad (4.24)$$

and the MSE of the detector can be expressed as

$$J = E \left[\left\| S - \hat{S} \right\|^2 \right] \quad (4.25)$$

Fig. 4.8 shows vector diagram depicting the relation between the original value, estimate and MSE. Here, e is the error given by

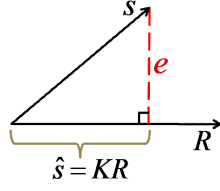


Figure 4.8: Vector diagram of MSE

$$e = S - \hat{S}. \quad (4.26)$$

Orthogonality principle [73] states that an estimator achieves MMSE if and only if the MSE is orthogonal to the observation. i.e. for J_{min} ,

$$\begin{aligned} e &\perp R \\ \Rightarrow E[eR^H] &= 0 \\ \Rightarrow E[(S - \hat{S})R^H] &= 0 \\ \Rightarrow E[(S - KR)R^H] &= 0 \\ \Rightarrow K &= E[SR^H]E[RR^H]^{-1}. \end{aligned} \quad (4.27)$$

4.3.1 MMSE System discription

The MMSE detector derived above estimates the baseband signal given by

$$\hat{S} = \mathbf{R}_{SR}\mathbf{R}_R^{-1}R \quad (4.28)$$

where \mathbf{R} denotes the correlation operator such that $\mathbf{R}_{SR} = E[SR^H]$ and $\mathbf{R}_R = E[RR^H]$.

Now, let us calculate it individually

$$\begin{aligned} \mathbf{R}_R &= E[RR^H] = E\left[\begin{bmatrix} r_0 \\ r_1^* \end{bmatrix} \begin{bmatrix} r_0^* & r_1 \end{bmatrix}\right] \\ &= E\begin{bmatrix} r_0r_0^* & r_0r_1 \\ r_1^*r_0^* & r_1^*r_1 \end{bmatrix} = \begin{bmatrix} \mathbf{R}_{R00} & \mathbf{R}_{R01} \\ \mathbf{R}_{R10} & \mathbf{R}_{R11} \end{bmatrix} \end{aligned} \quad (4.29)$$

substituting r_0 and r_1 , the correlation $\mathbf{R}_{R_{01}} = \mathbf{R}_{R_{10}} = 0$.

$$\begin{aligned}\mathbf{R}_{R_{00}} &= E [|s_0|^2 |h_0|^2 + |s_1|^2 |h_1|^2 + |n_0|^2] \\ &= \sigma_s^2 (|h_0|^2 + |h_1|^2) + \sigma_n^2 \\ &= \sigma_s^2 (\alpha_0^2 + \alpha_1^2) + \sigma_n^2.\end{aligned}\tag{4.30}$$

Similarly solving for $\mathbf{R}_{R_{11}}$, we get

$$\begin{aligned}\mathbf{R}_{R_{11}} &= E [|s_0|^2 |h_1|^2 + |s_1|^2 |h_0|^2 + |n_1|^2] \\ &= \sigma_s^2 (|h_0|^2 + |h_1|^2) + \sigma_n^2 \\ &= \sigma_s^2 (\alpha_0^2 + \alpha_1^2) + \sigma_n^2.\end{aligned}\tag{4.31}$$

Thus, $E [RR^H]$ becomes

$$\mathbf{R}_R = E [RR^H] = (\sigma_s^2 (\alpha_0^2 + \alpha_1^2) + \sigma_n^2) \mathbf{I}\tag{4.32}$$

Similarly, we calculate

$$\begin{aligned}\mathbf{R}_{SR} &= E [SR^H] = E \left[\begin{bmatrix} s_0 \\ s_1 \end{bmatrix} \begin{bmatrix} r_0^* & r_1 \end{bmatrix} \right] \\ &= E \begin{bmatrix} s_0 r_0^* & s_0 r_1 \\ s_1 r_0^* & s_1 r_1 \end{bmatrix} = \sigma_s^2 \begin{bmatrix} h_0^* & h_1 \\ h_1^* & -h_0 \end{bmatrix}\end{aligned}\tag{4.33}$$

Substituting the results of (4.32) and (4.33) in (4.27),

$$K = \frac{\sigma_s^2}{\sigma_s^2 (\alpha_0^2 + \alpha_1^2) + \sigma_n^2} \begin{bmatrix} h_0^* & h_1 \\ h_1^* & -h_0 \end{bmatrix}.\tag{4.34}$$

Thus, from (4.28), we get the mathematical expression of linear MMSE detector for a two branch MISO system as

$$\hat{S} = \frac{\sigma_s^2}{\sigma_s^2 (\alpha_0^2 + \alpha_1^2) + \sigma_n^2} \begin{bmatrix} h_0^* & h_1 \\ h_1^* & -h_0 \end{bmatrix} \begin{bmatrix} r_0 \\ r_1^* \end{bmatrix}\tag{4.35}$$

This is the simplest mathematical expression of MMSE for a two transmit diversity STBC system with perfect knowledge of the channel parameters and the CFO. In the next section, we will demonstrate the mathematical derivation of the MMSE detector with unknown CSI and unknown CFO respectively. The performance of the linear MMSE detector in terms of BER and computational complexity for different MIMO schemes is studied in [74] and for the case of multiple users, in [75].

4.3.2 MMSE detector with unknown CSI based upon CEP

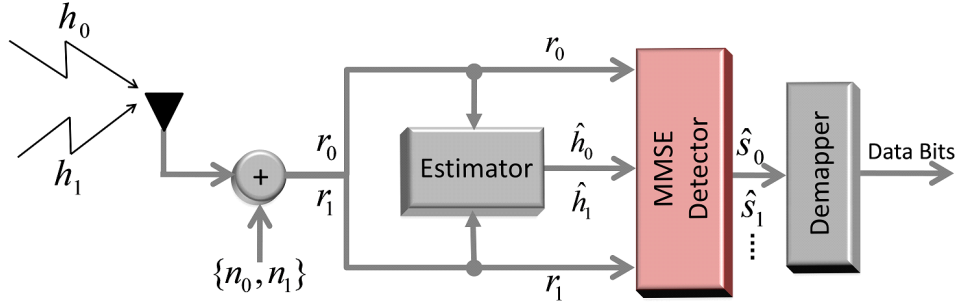


Figure 4.9: Generic block diagram of an MMSE detector with imperfect estimation of channel parameters and no CFO.

In the presence of erroneous estimates of the channel parameters as shown in Fig. (4.9), the MMSE detector derived above does not provide an optimal result. The constant factor in (4.34) is modified to

$$K = \frac{\sigma_s^2}{\sigma_s^2 (|\hat{h}_0|^2 + |\hat{h}_1|^2) + \sigma_n^2} \begin{bmatrix} \hat{h}_0^* & \hat{h}_1 \\ \hat{h}_1^* & -\hat{h}_0 \end{bmatrix}. \quad (4.36)$$

If we substitute the error in the channel parameters, the coefficient vector becomes

$$K = \frac{\sigma_s^2}{\sigma_s^2 (|h_0 + \varepsilon_0|^2 + |h_1 + \varepsilon_1|^2) + \sigma_n^2} \begin{bmatrix} h_0^* + \varepsilon_0^* & h_1 + \varepsilon_1 \\ h_1^* + \varepsilon_1^* & -h_0 - \varepsilon_0 \end{bmatrix}. \quad (4.37)$$

It is shown in [76–78] that MMSE detector with the above coefficient does not provide optimal detection. In the next section we will introduce unknown CFO to the system above.

4.3.3 MMSE detector with unknown CSI & CFO based upon CEP

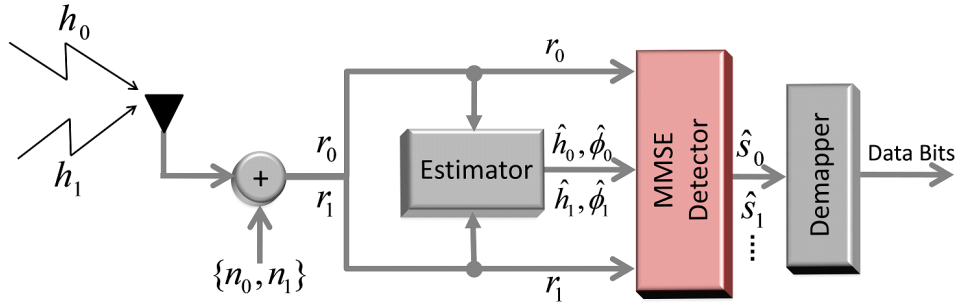


Figure 4.10: Generic block diagram of an unsynchronized MMSE detector with imperfect estimation of channel parameters.

Figure (4.10) shows a block diagram of an unsynchronized receiver incorporating CFO (3.17) into the system, the equation (4.30) modifies to

$$\begin{aligned} \mathbf{R}_{R_{00}} = \mathbf{R}_{R_{11}} &= E [|s_0|^2 |\hat{x}_0|^2 + |s_1|^2 |\hat{x}_1|^2 + |n_0|^2] \\ &= \sigma_s^2 (|\hat{x}_0|^2 + |\hat{x}_1|^2) + \sigma_n^2 \\ &= \sigma_s^2 (|h_0 + \varepsilon_0|^2 + |h_1 + \varepsilon_1|^2) + \sigma_n^2. \end{aligned} \quad (4.38)$$

Thus, $E [RR^H]$ stays same as $\sigma_s^2 (|h_0 + \varepsilon_0|^2 + |h_1 + \varepsilon_1|^2) + \sigma_n^2 \mathbf{I}$. However, the derivation in (4.33) changes to

$$\begin{aligned}
\mathbf{R}_{SR} &= E [SR^H] = \sigma_s^2 \begin{bmatrix} \hat{x}_{00}^* & \hat{x}_{11} \\ \hat{x}_{10}^* & -\hat{x}_{01} \end{bmatrix} \\
&= \sigma_s^2 \begin{bmatrix} (h_0^* + \varepsilon_0^*) e^{-j\hat{\phi}_{00}} & (h_1 + \varepsilon_1) e^{j\hat{\phi}_{11}} \\ (h_1^* + \varepsilon_1^*) e^{-j\hat{\phi}_{10}} & -(h_0 + \varepsilon_0) e^{j\hat{\phi}_{01}} \end{bmatrix}
\end{aligned} \tag{4.39}$$

Substituting this value, the MMSE coefficients can be written as

$$K = \frac{\sigma_s^2}{\sigma_s^2 (|h_0 + \varepsilon_0|^2 + |h_1 + \varepsilon_1|^2) + \sigma_n^2} \begin{bmatrix} (h_0^* + \varepsilon_0^*) e^{-j\hat{\phi}_{00}} & (h_1 + \varepsilon_1) e^{j\hat{\phi}_{11}} \\ (h_1^* + \varepsilon_1^*) e^{-j\hat{\phi}_{10}} & -(h_0 + \varepsilon_0) e^{j\hat{\phi}_{01}} \end{bmatrix} \tag{4.40}$$

which becomes very complex with the introduction of erroneous estimate of CFO as $\hat{\phi}_{i,k} = \phi_{i,k} + \epsilon_{i,k}$. The next chapter demonstrates the performance of all the detectors with unknown CSI and CFO estimation under a mismatch scenario and incorporating their estimation errors.

Chapter 5

Proposed detection schemes based upon the unknown CSI and CFO estimation errors

In the previous chapter, the effect of individual and both unknown CSI and CFO estimation errors has been discussed with detailed mathematical derivations and exhaustive simulations, for three of the most extensively used detection techniques in practical WC system which provides the best trade-off between performance and complexity. The simulation results demonstrate the degradation in the system performance under the mismatch scenario. In this chapter we focus on the unknown parameters which are estimated at the receiver and are not practically perfect.

In this chapter, we propose new detection algorithms, augmenting the conventional approaches discussed above, in the presence of CSI and CFO estimation errors. The extensive simulation curves exhibits remarkable improvement in terms of BER as compared to the conventional schemes under the same scenario derived in chapter 4.

5.1 Overview

It has been demonstrated in chapter 3 that, the unknown channel parameters and CFO are estimated using the overhead training data sequences called pilots. In the simulations in

section (3.3.2.1), it has been observed that by increasing the number of pilot symbols, increases the accuracy of estimation. However, pilot symbol length has to be kept low to save the bandwidth. Thus, with the limited pilot symbols, the estimator gets a partial knowledge of the unknown channel parameters.

This has opened the door for researchers to design an optimal detector with limited knowledge of these unknown parameters. Pioneering work has been done by Tarokh in [57, 79–81] by deriving variance of the unknown channel estimation error from the the limited pilot symbols. Tarokh proposed an ML decision metric for near optimal detection in the presence of channel estimation errors which improved the system performance. However, these decision metrics are derived with an assumption that the receiver frequency is perfectly synchronized with the transmit carrier frequency.

Besides accurate estimation and correction of CSI, another challenge to achieve an optimal detection of the data signal is to synchronize transmitter and receiver. We have already demonstrated the devastating effect of unsynchronized system adding CFO into their system, section 3.3.2.1, which has also motivated researchers over the period of time. Although most of the authors have considered CFO into their system model however, the detectors designed by them incorporated CFO as a deterministic value [61, 62] and not random. In practical systems, where CFO is random and is estimated, these detection algorithms will fail to provide optimal detection of the transmitted signal.

In the next section we will derive the variances of the estimation errors of the unknown CSI and CFO at the receiver.

5.2 Assumptions

Let us consider a two branch transmit diversity STBC system. The baseband signal transmitted from i -th antenna is given in (3.3). The channel parameters, channel estimates and the estimation errors are complex valued Gaussian RVs $h_i \sim \mathcal{N}(0, 1)$, $\hat{h}_i \sim \mathcal{N}(0, \sigma_{\hat{h}}^2)$ and $\varepsilon_i \sim \mathcal{N}(0, \sigma_{\varepsilon}^2)$ respectively. These three parameters are mathematically related by the form given in (3.11) and the relation between their variances can be easily written as

$$\begin{aligned}\sigma_{\hat{h}}^2 &= \sigma_h^2 + \sigma_{\varepsilon}^2 \\ &= 1 + \sigma_{\varepsilon}^2.\end{aligned}\tag{5.1}$$

It has been already shown in [79, 80], that introducing the correlation between the original channel parameter h_i and the estimate \hat{h}_i into the detection algorithm shows considerable improvement in the system performance. Using the results in [79], the correlation coefficient can be given as

$$\rho = \frac{1}{\sqrt{1 + \sigma_{\varepsilon}^2}}.\tag{5.2}$$

Now, let us consider the system with both CSI and CFO. Here, the baseband signal from the i -th transmit antenna is given in (3.17). It is rewritten here for the ease of referring by the mathematical derivations explained ahead in the chapter.

$$r_k = \sum_{i=0}^{m-1} h_i e^{j\phi_{i,k}} s_{i,k} \sqrt{E_s} + n_k\tag{5.3}$$

The CAFO parameters, CAFO estimates and the estimation errors are Gaussian RVs $\phi_{i,k} \sim \mathcal{N}(0, \sigma_{\phi}^2)$, $\hat{\phi}_{i,k} \sim \mathcal{N}(0, \sigma_{\hat{\phi}}^2)$ and $\varepsilon_{i,k} \sim \mathcal{N}(0, \sigma_{\varepsilon}^2)$ respectively. From (3.19), the relation between the variances of these parameters can be easily given as

$$\sigma_{\hat{\phi}}^2 = \sigma_{\phi}^2 + \sigma_{\varepsilon}^2.\tag{5.4}$$

The correlation coefficient between the original CAFO $\phi_{i,k}$ and the estimate $\hat{\phi}_{i,k}$ is calculated as

$$\begin{aligned}\lambda &= \frac{E \left[\phi_{i,k} \hat{\phi}_{i,k} \right]}{\sqrt{\sigma_{\phi}^2 \sigma_{\hat{\phi}}^2}} \\ &= \sqrt{1 - \frac{\sigma_{\epsilon}^2}{\sigma_{\phi}^2}}\end{aligned}\tag{5.5}$$

Using these assumptions, new detection algorithms will be derived incorporating the estimation error of the unknown CSI and CFO. The derivations for the algorithms based of ML detector, linear MRC combiner and MMSE is shown in section 5.3, section 5.4 and section 5.5 respectively. We will also investigate their BER performance for Alamouti's two branch transmit diversity STBC system.

5.3 Proposed ML detector

Tarokh et al. [57, 79] proposed a detection metric using Maximum Likelihood detection technique, which is one of the most widely used detectors in WC systems. His metric incorporated imperfect channel estimates, derived primarily for space time coded MIMO systems however, it is now used [58] as a generalized metric for all MIMO systems.

Let us derive the ML detector Tarokh's way. Here, the original channel parameter h_i and its estimate \hat{h}_i are taken as bi-variate Gaussian distributed. Thus, the expectation of h_i conditioned on \hat{h}_i is

$$E \left[h_i | \hat{h}_i \right] = \frac{\rho \hat{h}_i}{\sigma_{\hat{h}}}\tag{5.6}$$

and the variance is

$$Var \left[h_i | \hat{h}_i \right] = 1 - |\rho|^2.\tag{5.7}$$

Using the relation in (3.3), the expectation of the received signal r_k conditioned on \hat{h}_i is calculated as

$$E \left[r_k | \hat{h}_i \right] = \frac{\rho \hat{h}_i s_{i,k} \sqrt{E_s}}{\sigma_{\hat{h}}}\tag{5.8}$$

and the variance as

$$\text{Var} [r_k | \hat{h}_i] = N_0 + (1 - |\rho|^2) E_s |s_{i,k}|^2. \quad (5.9)$$

Taking negative logarithm of the likelihood function, the decision metric for a two branch MISO system was derived as

$$s_{i,k} \triangleq \arg \min_{s \in \mathcal{C}} \sum_{k=0}^1 \left(\frac{\left| r_k - \sum_{i=0}^1 \frac{\rho \hat{h}_i s_{i,k} \sqrt{E_s}}{\sigma_{\hat{h}}} \right|^2}{N_0 + (1 - |\rho|^2) E_s |s_{i,k}|^2} + \ln (N_0 + (1 - |\rho|^2) E_s |s_{i,k}|^2) \right) \quad (5.10)$$

and for equal energy modulations like PSK, it was reduced to

$$s_{i,k} \triangleq \arg \min_{s \in \mathcal{C}} \sum_{k=0}^1 \left| r_k - \sum_{i=0}^1 \frac{\rho \hat{h}_i \sqrt{E_s} s_{i,k}}{\sigma_{\hat{h}}} \right|^2. \quad (5.11)$$

Now, let us consider a system with CFO and the estimate of CAFO available to the receiver is $\hat{\phi}_{i,k}$. With CFO introduced into the signal given by (3.17), we can say that r_k has no more a Normal distribution. However, it displays a Gaussian like behavior [67] and hence, we assume the conditional pdf of r_k to be Gaussian. Since r_k depends upon $s_{i,k}$, \hat{h}_i and $\hat{\phi}_{i,k}$ we can obtaine maximizing the MAP probability given as

$$s_{i,k} \triangleq \arg \max_{s \in \mathcal{C}} \left\{ P \left(s_{i,k} | r_k, \hat{h}_i, \hat{\phi}_{i,k} \right) \right\}. \quad (5.12)$$

This leads to maximizing the likelihood function,

$$s_{i,k} \triangleq \arg \max_{s \in \mathcal{C}} \left\{ P \left(r_k | s_{i,k}, \hat{h}_i, \hat{\phi}_{i,k} \right) \right\}. \quad (5.13)$$

Thus, considering r_k as gaussian, the optimal detection of the transmitted signal is obtained by taking negative logarithm of the likelihood function.

$$s_{i,k} \triangleq \arg \max_{s \in \mathcal{C}} \sum_{k=0}^1 \left(\ln \left(\text{Var} \left[r_k | \hat{h}_i, \hat{\phi}_{i,k} \right] \right) + \frac{\left| r_k - \sum_{i=0}^1 E \left[r_k | \hat{h}_i, \hat{\phi}_{i,k} \right] \right|^2}{2 \text{Var} \left[r_k | \hat{h}_i, \hat{\phi}_{i,k} \right]} \right) \quad (5.14)$$

The values of $E \left[r_k | \hat{h}_i, \hat{\phi}_{i,k} \right]$ and $\text{Var} \left[r_k | \hat{h}_i, \hat{\phi}_{i,k} \right]$ are computed elaborately in Appendix A. For modulations with equal energy like PSK, the decision metric can be modified to

$$\begin{aligned} s_{i,k} &\triangleq \arg \max_{s \in \mathcal{C}} \sum_{k=0}^1 \left| r_k - \sum_{i=0}^1 E \left[r_k | \hat{h}_i, \hat{\phi}_{i,k} \right] \right|^2 \\ &= \sum_{k=0}^1 \left| r_k - \sum_{i=0}^1 \frac{\rho \sqrt{E_s} \sum_{i=1}^n \hat{h}_i \hat{s}_{i,k}}{\sqrt{2} \sigma_{\hat{h}}} e^{\left(\frac{j \lambda \hat{\phi}_{i,k}}{\sigma_{\hat{\phi}}} - \frac{(1 - \lambda^2)}{2} \right)} \right|^2 \end{aligned} \quad (5.15)$$

This novel ML decision metric in the presence of CSI and CFO estimation error for a two branch MISO can be further generalized for a m -branch MISO as

$$s_{i,k} \triangleq \arg \max_{s \in \mathcal{C}} \sum_{k=0}^{m-1} \left(\ln \left(\text{Var} \left[r_k | \hat{h}_i, \hat{\phi}_{i,k} \right] \right) + \frac{\left| r_k - \sum_{i=0}^{m-1} E \left[r_k | \hat{h}_i, \hat{\phi}_{i,k} \right] \right|^2}{2 \text{Var} \left[r_k | \hat{h}_i, \hat{\phi}_{i,k} \right]} \right) \quad (5.16)$$

and for m -branch MISO PSK modulations as

$$s_{i,k} \triangleq \arg \max_{s \in \mathcal{C}} \sum_{k=0}^{m-1} \left| r_k - \sum_{i=0}^{m-1} \frac{\rho \sqrt{E_s} \hat{h}_i s_{i,k}}{\sigma_{\hat{h}}} e^{\left(\frac{j \lambda \hat{\phi}_{i,k}}{\sigma_{\hat{\phi}}} - \frac{(1 - \lambda^2)}{2} \right)} \right|^2. \quad (5.17)$$

5.3.1 Convergence to conventional ML detector

To evaluate the correctness of the proposed ML detection metric for STBC, consider two special cases.

1. **Perfect CSI and CFO estimator:** Consider that the receiver has a perfect Carrier Frequency Offset estimator. Thus from equation (3.17) it implies, $\hat{\phi}_{i,k} = \phi_{i,k}$ or the CFO error $\epsilon_{i,k}$ equals to zero. Thus the correlation coefficient λ becomes one and $\sigma^2_{\hat{\phi}} = \sigma^2_{\phi} = 1$. Substituting in (5.17), we get

$$s_{i,k} \triangleq \arg \max_{s \in \mathcal{C}} \sum_{k=0}^{m-1} \left| r_k - \sum_{i=0}^{m-1} \frac{\rho \sqrt{E_s} \hat{h}_i s_{i,k}}{\sigma_{\hat{h}}} e^{(0+j\phi_{i,k})} \right|^2. \quad (5.18)$$

Tarokh's metric did not take into account CFO, therefore his system model follows the relation in (5.11). Thus the reduced form of the proposed metric (5.18) shows that Tarokh's metric without the CFO, is a special case of the new proposed decision metric (5.17) with CFO.

2. **Perfect CSI estimator and no CFO:** To evaluate the correctness of the proposed ML detection matrix for STBC, with the conventional ML detector without CFO $\phi = 0$, let us consider that the receiver has a perfect channel estimator. Thus from equation (3.11) it implies, $\hat{h}_i = h_i$ or the channel error ϵ_i equals to zero. Thus the correlation coefficient ρ becomes one and $\sigma^2_{\hat{h}} = \sigma^2_h = 1$. Substituting in (5.18), we get

$$s_{i,k} \triangleq \arg \max_{s \in \mathcal{C}} \sum_{k=0}^{m-1} \left| r_k - \sum_{i=0}^{m-1} \sqrt{E_s} h_i s_{i,k} \right|^2. \quad (5.19)$$

which is the same as (4.6).

5.4 Proposed MRC detector

We have already expressed the MRC linear combiner mathematical form $\tilde{S} = W^H R = W^H (XS + N)$ in (3.21). In the proposed MRC combiner form, when the CSI and CFO are unknown and are estimated at the receiver, we take

$$X_{optimal} = E \left[X | \hat{h}_i, \hat{\phi}_{i,k} \right] \quad (5.20)$$

as the expectations of individual elements X conditioned on the estimated parameters \hat{h}_i and $\hat{\phi}_{i,k}$. Therefore, the instantaneous output SNR of the combiner as given in [73], can be written as

$$\begin{aligned} SNR &= \frac{E \left[|W^H X S|^2 \right]}{E \left[|W^H N|^2 \right]}. \\ &= \frac{E \left[|S|^2 \right] \left| W^H E \left[X | \hat{h}_i, \hat{\phi}_{i,k} \right] \right|^2}{E \left[|N|^2 \right] |W^H|^2} \end{aligned} \quad (5.21)$$

By Cauchy Schwartz inequality it is shown that SNR is maximum when $W = E \left[X | \hat{h}_i, \hat{\phi}_{i,k} \right]$. Thus, equation (5.20) can be rewritten as

$$\tilde{S} = E \left[X | \hat{h}_i, \hat{\phi}_{i,k} \right]^H R \quad (5.22)$$

Expanding R and X using (3.4) and (3.21) respectively, (5.22) becomes

$$\begin{bmatrix} \tilde{s}_0 \\ \tilde{s}_1 \end{bmatrix} = E \begin{bmatrix} x_{00} | \hat{h}_0, \hat{\phi}_{00} & x_{10} | \hat{h}_1, \hat{\phi}_{10} \\ x_{11} | \hat{h}_1, \hat{\phi}_{11} & x_{01} | \hat{h}_0, \hat{\phi}_{01} \end{bmatrix}^H \begin{bmatrix} r_0 \\ r_1^* \end{bmatrix}. \quad (5.23)$$

Assuming the channel coefficients and the CFO are independent of each other, we can write

$$E[x_{i,k} | \hat{h}_i, \hat{\phi}_{i,k}] = E[h_i | \hat{h}_i] E[e^{j\phi_{i,k}} | \hat{\phi}_{i,k}]. \quad (5.24)$$

Substituting the mathematical derivation of $E[e^{j\phi_{i,k}} | \hat{\phi}_{i,k}]$ from Appendix A and $E[h_i | \hat{h}_i]$ using equation (5.6) into (5.23),

$$\begin{bmatrix} \tilde{s}_0 \\ \tilde{s}_1 \end{bmatrix} = \Upsilon \begin{bmatrix} \hat{h}_0^* e^{\left(\frac{-j\lambda\hat{\phi}_{00}}{\sigma_\phi^2} \right)} & \hat{h}_1 e^{\left(\frac{j\lambda\hat{\phi}_{11}}{\sigma_\phi^2} \right)} \\ \hat{h}_1^* e^{\left(\frac{-j\lambda\hat{\phi}_{10}}{\sigma_\phi^2} \right)} & -\hat{h}_0 e^{\left(\frac{j\lambda\hat{\phi}_{01}}{\sigma_\phi^2} \right)} \end{bmatrix} \begin{bmatrix} r_0 \\ r_1^* \end{bmatrix} \quad (5.25)$$

where $\Upsilon = \rho e^{-\frac{(1-\lambda^2)}{2}} / \sigma_{\hat{h}}$.

5.4.1 ML Detection Methodology

The proposed ML detection cost function in the presence of estimation errors at the receiver is to choose \hat{s}_i from a set of codewords. The ML detector in (3.9) modifies to

$$\begin{aligned} & \left(\left| E \left[x_{00}^* | \hat{h}_0, \hat{\phi}_{00} \right] \right|^2 + \left| E \left[x_{11} | \hat{h}_1, \hat{\phi}_{11} \right] \right|^2 - 1 \right) |\hat{s}_i|^2 \\ & \quad + d^2(\tilde{s}_0, \hat{s}_i) \\ & \left(\left| E \left[x_{10}^* | \hat{h}_1, \hat{\phi}_{10} \right] \right|^2 + \left| E \left[x_{01} | \hat{h}_0, \hat{\phi}_{01} \right] \right|^2 - 1 \right) |\hat{s}_i|^2 \\ & \quad + d^2(\tilde{s}_1, \hat{s}_i) \end{aligned} \quad (5.26)$$

for \tilde{s}_0 and \tilde{s}_1 and for all values of \hat{s}_i . Using the values from (5.25), (5.26) becomes

$$\left(\left| \Upsilon \hat{h}_0 \right|^2 + \left| \Upsilon \hat{h}_1 \right|^2 - 1 \right) |\hat{s}_i|^2 + d^2(\tilde{s}, \hat{s}_i). \quad (5.27)$$

For PSK modulation, the ML detector remains $d^2(\tilde{s}, \hat{s}_i)$.

5.4.2 Convergence to conventional MRC detector

To evaluate the convergence of the proposed MRC detection scheme to the conventional MRC scheme, let us consider two special cases.

1. **Perfect CSI and CFO estimator:** The conventional MRC given in (3.5), assumes that the both the CSI and CFO are known to the receiver. Let us assume a similar case for the new derived MRC which means, both the estimators of the CSI and CFO at the receiver are perfect i.e. $\hat{h}_i = h_i$ and $\hat{\phi}_{i,k} = \phi_{i,k}$. The correlation coefficient between the original CSI h_i and its estimate \hat{h}_i , $\rho = 1$. Similarly for CAFO, the correlation coefficient between $\phi_{i,k}$ and $\hat{\phi}_{i,k}$, $\lambda = 1$. Substituting these values in (5.25) and (5.27), $\Upsilon = \rho e^{-\frac{(1-\lambda^2)}{2}} / \sigma_{\hat{h}} = 1$ and we get the form of the conventional MRC with known CSI and CFO which is

$$\begin{bmatrix} \tilde{s}_0 \\ \tilde{s}_1 \end{bmatrix} = \begin{bmatrix} h_0^* e^{-j\phi_{00}} & h_1 e^{j\phi_{11}} \\ h_1^* e^{-j\phi_{10}} & -h_0 e^{j\phi_{01}} \end{bmatrix} \begin{bmatrix} r_0 \\ r_1^* \end{bmatrix}. \quad (5.28)$$

2. **Perfect CSI estimator and no CFO:** For a case of a perfect synchronized transmitter receiver with no CFO, this becomes equivalent to (3.5) and the conventional ML detector given in (3.9) respectively. Thus, it can be shown that the new derived combiner can be reduced to the conventional MRC for the ideal case of perfect synchronization, i.e. no CFO and perfect CSI estimators.

5.5 Proposed MMSE detector

Linear MMSE detectors described in section 4.3 demonstrated the degraded performance incorporating unknown CSI and CFO. In this section we will derive the proposed MMSE detector whose main objective is to minimize the cost function $J = E \left[(s_i - \hat{s}_i)^2 | \hat{h}_i, \hat{\phi}_{i,k} \right]$.

A generalized linear estimator can be written in the form

$$\hat{S} = \mathbf{R}_{SR} \mathbf{R}_R^{-1} R \quad (5.29)$$

where \hat{S} is the signal after detection, \mathbf{R} denotes the correlation operator such that $\mathbf{R}_{SR} = E [SR^H]$, $\mathbf{R}_R = E [RR^H]$ and $R = [r_0 \ r_1^*]^T$ are the received signals. The system in this scenario does not have the knowledge of the CSI and CFO. Thus, the imperfect estimates of CSI \hat{h}_i and CAFO $\hat{\phi}_{i,k}$ are available to the receiver. Let us assume

$$\hat{x}_{i,k} = \hat{h}_i e^{j\hat{\phi}_{i,k}} \quad (5.30)$$

Calculating these parameters individually,

$$\begin{aligned} \mathbf{R}_R &= E \left[\begin{bmatrix} r_0 \\ r_1^* \end{bmatrix} \begin{bmatrix} r_0^* & r_1 \end{bmatrix} \right] \\ &= E \begin{bmatrix} r_0 r_0^* & r_0 r_1 \\ r_1^* r_0^* & r_1^* r_1 \end{bmatrix} = \begin{bmatrix} \mathbf{R}_{R_{00}} & \mathbf{R}_{R_{01}} \\ \mathbf{R}_{R_{10}} & \mathbf{R}_{R_{11}} \end{bmatrix} \end{aligned} \quad (5.31)$$

substituting r_0 and r_1 , the correlation $\mathbf{R}_{R_{01}} = \mathbf{R}_{R_{10}} = 0$.

$$\begin{aligned}
\mathbf{R}_{R_{00}} &= E \left[|s_0|^2 |x_0|^2 + |s_1|^2 |x_1|^2 + |n_0|^2 \right] \\
&= E \left[|x_{00}|^2 \hat{h}_0, \hat{\phi}_{00} \right] + E \left[|x_{10}|^2 \hat{h}_1, \hat{\phi}_{10} \right] + \sigma_n^2 \\
&= E \left[h_0^2 | \hat{h}_0 \right] + E \left[h_1^2 | \hat{h}_1 \right] + \sigma_n^2 \\
&= 2(1 - \rho^2) + \frac{\rho^2 \left| \hat{h}_0 \right|^2}{\sigma_{\hat{h}}^2} + \frac{\rho^2 \left| \hat{h}_1 \right|^2}{\sigma_{\hat{h}}^2} + \sigma_n^2. \\
&= \Lambda
\end{aligned} \tag{5.32}$$

Similarly we can solve for $\mathbf{R}_{R_{11}}$ and substitute Λ . Thus,

$$\begin{aligned}
\mathbf{R}_{R_{11}} &= E \left[|s_0|^2 |x_{11}|^2 + |s_1|^2 |x_{01}|^2 + |n_1|^2 \right] \\
&= E \left[|x_{11}|^2 \hat{h}_1, \hat{\phi}_{11} \right] + E \left[|x_{01}|^2 \hat{h}_0, \hat{\phi}_{01} \right] + \sigma_n^2 \\
&= \Lambda
\end{aligned} \tag{5.33}$$

Using the above results, \mathbf{R}_R can be expressed as ΛI . Thus \mathbf{R}_R^{-1} can be written as $\Lambda^{-1} I$.

Similarly,

$$\begin{aligned}
\mathbf{R}_{SR} &= E \begin{bmatrix} s_0 r_0^* & s_0 r_1 \\ s_1 r_0^* & s_1 r_1 \end{bmatrix} \\
&= E \left[|s|^2 \right] \begin{bmatrix} E[x_{00}^* | \hat{h}_0, \hat{\phi}_{00}] & E[x_{11} | \hat{h}_1, \hat{\phi}_{11}] \\ E[x_{10}^* | \hat{h}_1, \hat{\phi}_{10}] & -E[x_{01} | \hat{h}_0, \hat{\phi}_{01}] \end{bmatrix}
\end{aligned} \tag{5.34}$$

Substituting \mathbf{R}_{SR} (5.34) and \mathbf{R}_R^{-1} in (5.29) we get

$$\begin{bmatrix} \hat{s}_0 \\ \hat{s}_1 \end{bmatrix} = \frac{1}{\Lambda} \begin{bmatrix} E[x_{00}^* | \hat{h}_0, \hat{\phi}_{00}] & E[x_{11} | \hat{h}_1, \hat{\phi}_{11}] \\ E[x_{10}^* | \hat{h}_1, \hat{\phi}_{10}] & -E[x_{01} | \hat{h}_0, \hat{\phi}_{01}] \end{bmatrix} \begin{bmatrix} r_0 \\ r_1^* \end{bmatrix} \tag{5.35}$$

Again assuming the channel coefficients and the CFO are independent of each other, we

can write

$$E[x_{i,k}|\hat{h}_i, \hat{\phi}_{i,k}] = E[h_i|\hat{h}_i] E[e^{j\phi_{i,k}}|\hat{\phi}_{i,k}]. \quad (5.36)$$

Substituting the mathematical derivation of $E[e^{j\phi_{i,k}}|\hat{\phi}_{i,k}]$ from Appendix A and $E[h_i|\hat{h}_i]$ using equation (5.6) into (5.35),

$$\begin{bmatrix} \tilde{s}_0 \\ \tilde{s}_1 \end{bmatrix} = \frac{\Upsilon}{\Lambda} \begin{bmatrix} \hat{h}_0^* e^{\left(\frac{-j\lambda\hat{\phi}_{00}}{\sigma_\phi^2}\right)} & \hat{h}_1 e^{\left(\frac{j\lambda\hat{\phi}_{11}}{\sigma_\phi^2}\right)} \\ \hat{h}_1^* e^{\left(\frac{-j\lambda\hat{\phi}_{10}}{\sigma_\phi^2}\right)} & -\hat{h}_0 e^{\left(\frac{j\lambda\hat{\phi}_{01}}{\sigma_\phi^2}\right)} \end{bmatrix} \begin{bmatrix} r_0 \\ r_1^* \end{bmatrix} \quad (5.37)$$

where $\Upsilon = \rho e^{-\frac{(1-\lambda^2)}{2}} / \sigma_{\hat{h}}$.

5.5.1 Convergence to conventional MMSE detector

Here, we consider two special cases for the novel MMSE detector derived above.

1. **Perfect CSI and CFO estimator:** Here we assume that the estimator for both CSI and CFO are perfect i.e. $\hat{h}_i = h_i$ and $\hat{\phi}_{i,k} = \phi_{i,k}$ respectively. This makes the values of the respective correlation coefficients unity i.e. $\rho = \lambda = 1$ then $\Upsilon = 1$ and $\Lambda = |\hat{h}_0|^2 + |\hat{h}_1|^2 + \sigma_n^2$. It is evident now, that the variances of the CSI and CFO estimates are $\sigma_{\hat{h}}^2 = \sigma_h^2$ and $\sigma_{\hat{\phi}}^2 = \sigma_\phi^2$ respectively. Substituting these values in (5.37), we get

$$\begin{bmatrix} \tilde{s}_0 \\ \tilde{s}_1 \end{bmatrix} = \frac{1}{|h_0|^2 + |h_1|^2 + \sigma_n^2} \begin{bmatrix} h_0^* e^{(-j\phi_{00})} & h_1 e^{(j\phi_{11})} \\ h_1^* e^{(-j\phi_{10})} & -h_0 e^{(j\phi_{01})} \end{bmatrix} \begin{bmatrix} r_0 \\ r_1^* \end{bmatrix} \quad (5.38)$$

which is the form of conventional MMSE detector in the presence of perfect estimation at the receiver.

2. **Perfect CSI estimator and no CFO:** Let us make the similar assumption as above. However, now we assume a system in the absence of CFO. This means $\hat{\phi}_{i,k} = \phi_{i,k} =$

0, $\sigma_{\hat{\phi}}^2 = \sigma_{\phi}^2 = 0$ and $\lambda = 1$. Thus, the MMSE detector in (5.38) becomes

$$\begin{bmatrix} \tilde{s}_0 \\ \tilde{s}_1 \end{bmatrix} = \frac{1}{\alpha_0^2 + \alpha_1^2 + \sigma_n^2} \begin{bmatrix} h_0^* & h_1 \\ h_1^* & -h_0 \end{bmatrix} \begin{bmatrix} r_0 \\ r_1^* \end{bmatrix} \quad (5.39)$$

This is the form of a conventional MMSE detector for an ideal scenario.

Thus, it is shown that the proposed MMSE detection algorithm is a general form for practical systems and the conventional algorithms are its special cases.

5.6 Simulation analysis

In this section, the performance of the proposed detection algorithms derived above is demonstrated by simulations performed in Matlab. The system model is assumed to be a two branch transmit diversity STBC which is mathematically expressed in (3.17). The AWGN as assumed earlier, is considered a complex valued zero mean Gaussian RV with power spectral density $N_0/2$ per dimension which depends on the SNR and the modulation scheme.

$$\begin{aligned} SNR = \Gamma &= \frac{E_b}{N_0} \\ &= \frac{E_s}{R_m R_c N_0} \\ \Rightarrow N_0 &= \frac{E_s}{R_m R_c \Gamma}, \end{aligned} \quad (5.40)$$

where E_s is the symbol energy, $R_m = \log_2(M)$ for M -ary modulation scheme and R_c is the code rate of the system. For modulation schemes having equal energy constellations like PSK, $E_s = 1$. Here, we assume no coding for the system and so $R_c = 1$.

Similar to the assumptions made for the derivations given above, the channel parameters $h_i \sim \mathcal{N}(0, 1)$ and the channel estimates $\hat{h}_i \sim \mathcal{N}(0, \sigma_{\hat{h}}^2)$ are zero mean Gaussian RV with variance unity and $\sigma_{\hat{h}}^2$ respectively. The channel estimation error variance is a function

of the AWGN variance and pilot length as given in (3.16). For the simulations shown in this section, the pilot length is assumed to be 2.

Regardless to the type of estimator used, the original CFO is mathematically related to its estimate and the estimation error is given in (3.19). The original value of CFO $\phi_{i,k} \sim \mathcal{N}(0, \sigma_\phi^2)$ and its estimate $\hat{\phi}_{i,k} \sim \mathcal{N}(0, \sigma_{\hat{\phi}}^2)$ are zero mean Gaussian RV with variance σ_ϕ^2 and $\sigma_{\hat{\phi}}^2$ respectively. The simulations are performed with varying values of the CFO estimation error variance which is assumed to be multiple of the noise variance

$$\sigma_\epsilon^2 = M\sigma_n^2 \quad (5.41)$$

where M takes the value 1, 4 and 9.

Complex data symbols, depending upon the type of modulation scheme are used for simulations. To achieve the best average of BER to a given value of SNR, 10^4 frames of symbols are considered having a frame length of 130 symbols. The performance analysis is performed by plotting the average BER against its respective SNR. A comparison is made between the proposed algorithms derived in this chapter and their respective conventional forms discussed in Chapter 4 under the mismatch scenario.

Fig. 5.1 demonstrates the performance of the three proposed detectors compared with the conventional detector for 4-PSK modulation scheme with error variance equal to the noise variance. Here all the three proposed detection techniques perform similar. Hence, we can deduce that the all the three proposed detectors are near optimal detectors.

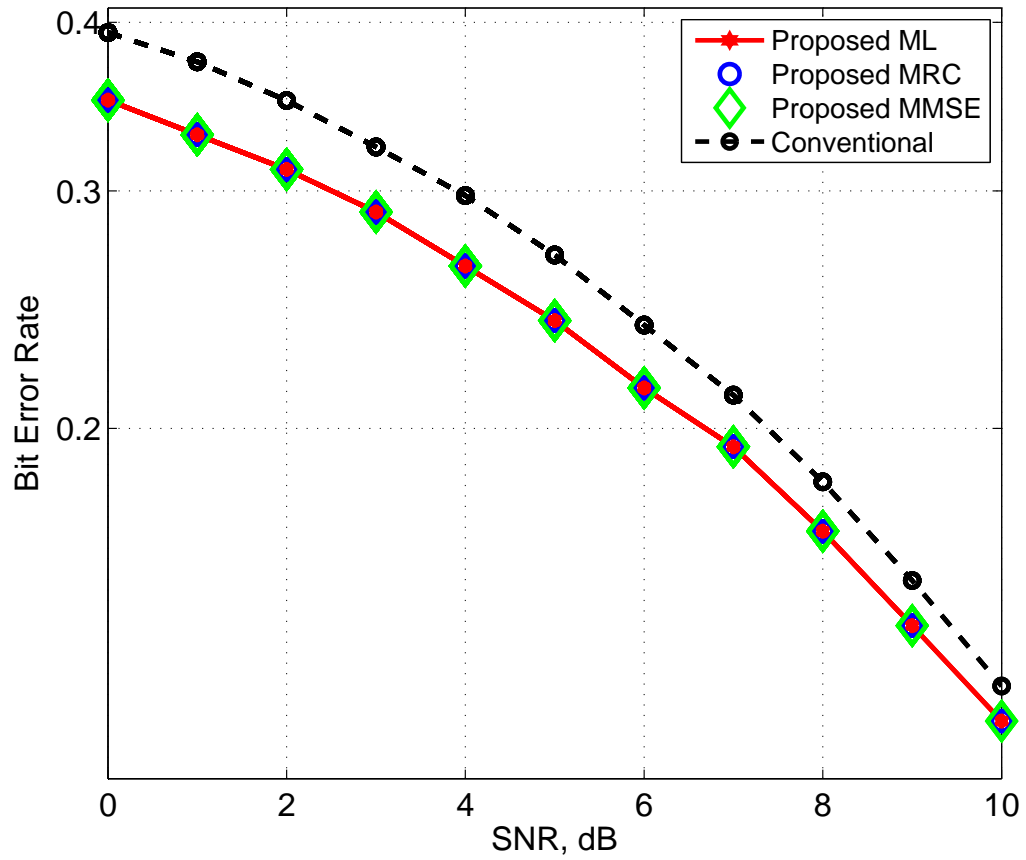


Figure 5.1: Performance of 4-PSK STBC system with proposed detector.

The future simulations are performed taking any one detection technique to compare with the conventional techniques for different cases.

Fig. 5.2 shows the performance simulation for 4-PSK compared with the conventional method for different values of error variances. It is shown that at $M = 1$ the proposed metric performs 1.5 dB better than the conventional metric, which is increased up to 4 dB at $M = 9$. It can be easily said that the proposed metric performs better than the conventional metric. Similar dB gain can be noticed in the higher modulation schemes as shown in Fig. 5.3 for 8-PSK and 16-PSK STBC system.

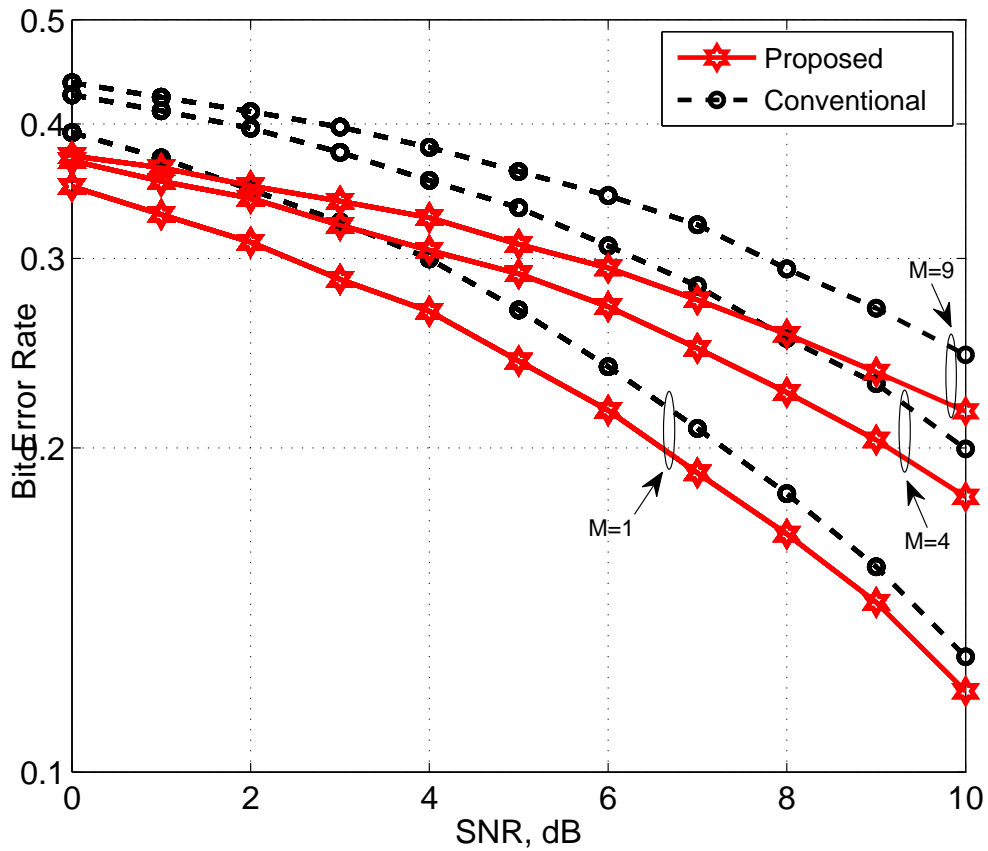
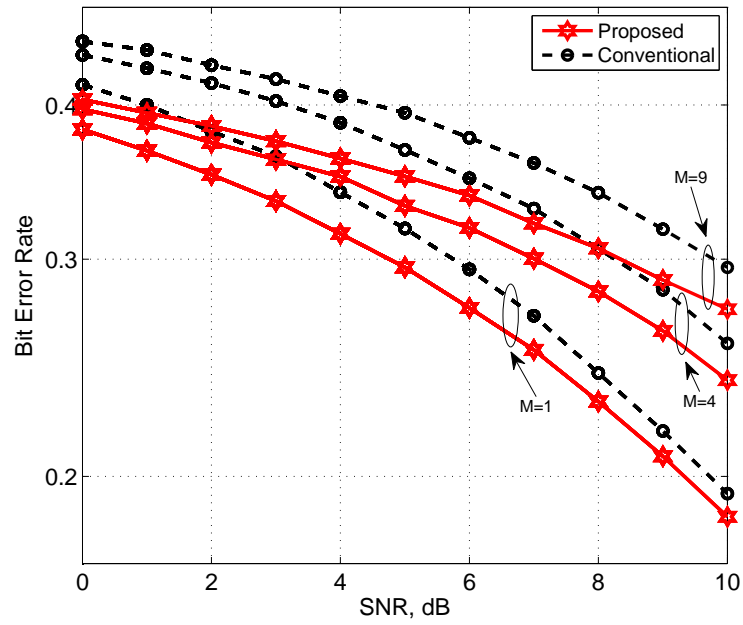
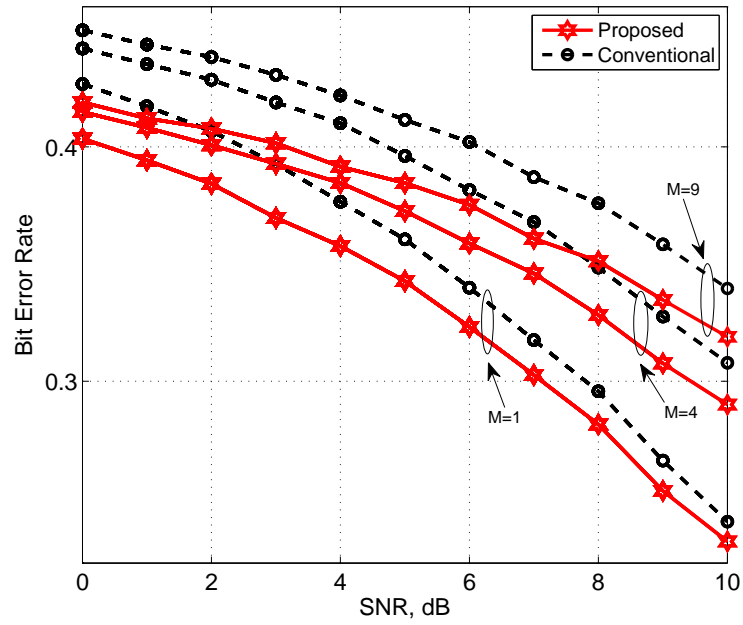


Figure 5.2: Performance of 4-PSK STBC system with proposed detector.



(a) 8-PSK



(b) 16-PSK

Figure 5.3: Performance of M-PSK STBC system with proposed detector.

PSK modulation schemes have equal energy in each constellation. In order to consider the case for unequal energy for each constellation, the performance simulation is repeated for 4-QAM given in Fig. 5.4, 16-QAM and 64-QAM in Fig. 5.5. The performance of 4-QAM is similar to that of QPSK and the proposed detector provides 1.5 dB and 4 dB gain in SNR for $M = 1$ and $M = 9$ respectively.

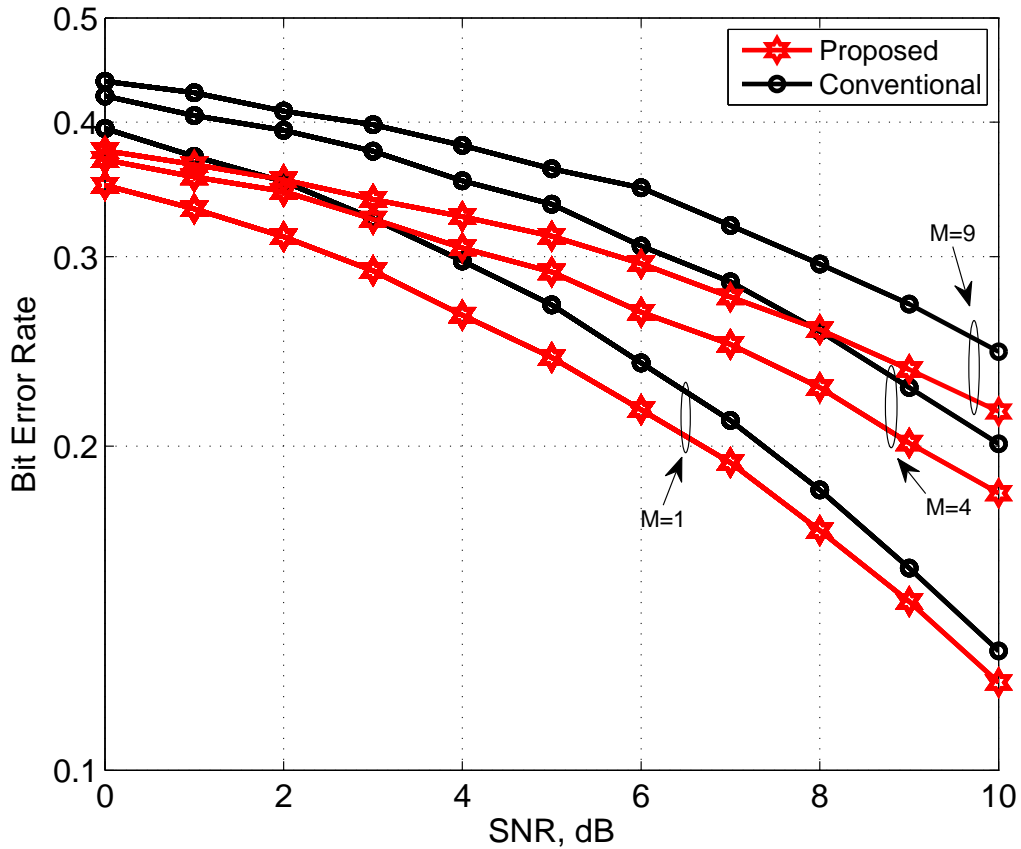
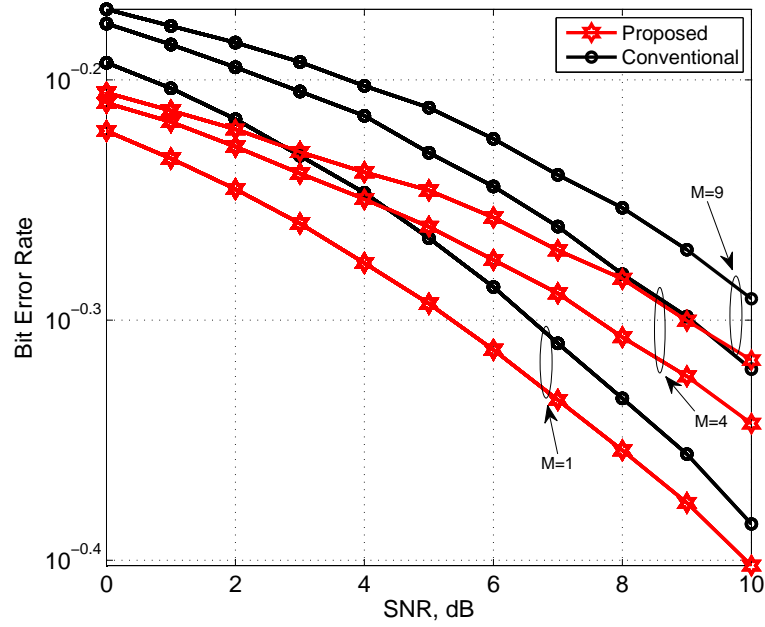
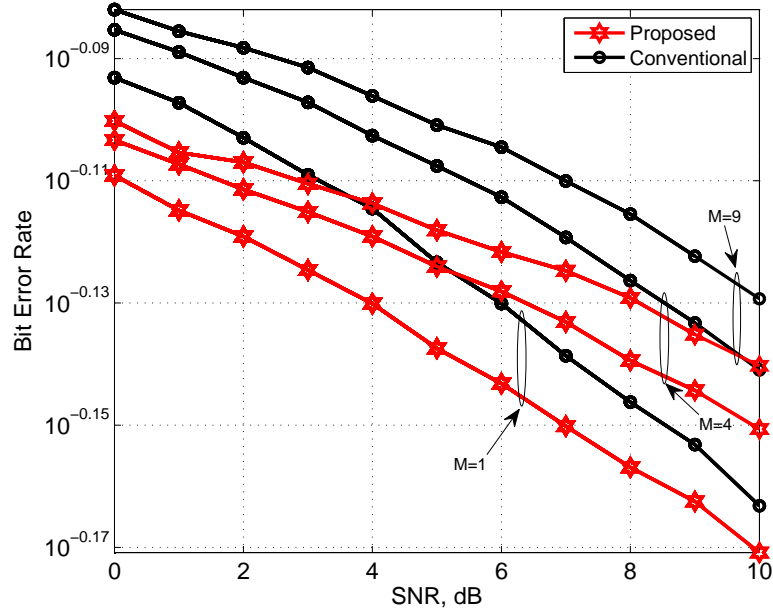


Figure 5.4: Performance of 4-QAM STBC system with proposed detector.



(a) 16-QAM



(b) 64-QAM

Figure 5.5: Performance of M-QAM STBC system with proposed detector.

We have noticed from the simulation graphs that all the three detectors perform similar in terms of BER as compared to the conventional detectors for different variances of the erroneous estimates of the unknown parameters. The simulation graphs demonstrate that the more the error variance of the estimator, the more accurate is the proposed detector in terms of BER, towards the optimal estimation of the transmitted signal as compared to the conventional detector. From other point of view, the proposed detectors have comparatively lower BER at lower SNRs than the conventional metrics.

As the three proposed detectors perform similar, the important issue is to determine the factor to compare between all the three for the best possible detectors. Comparing the computational complexity for each of the three proposed detectors, the first ML detector works by choosing a symbol from a set of given symbols in such a way, that it has maximum probability of being transmitted conditioned on the received signal and the channel parameters. This algorithm involves multiple iterations and exponential complexity. The second detection scheme involves MRC and ML decision block, which incorporates the complexity of a linear model and the iterative model. The third detector is based on linear MMSE detection scheme assumes a simple linear model and thus has the least computational and time complexity among all the three.

Chapter 6

Conclusion and Future Work

This thesis emphasizes the unexploited challenges in an unsynchronized STBC system. In Chapter 3, we have reviewed the background of STBC and investigated the effects of unknown parameters on the performance of the system. This research involves the unknown Rayleigh fading channel parameters and the CFO at the receiver. Chapter 4 exhibits the three powerful detection schemes that are most commonly used for practical purposes. These are

- Maximum Likelihood Detector (ML)
- Maximal Ratio Combiner (MRC)
- Minimum Mean Square Error Detector (MMSE).

The first detector involves the classical ML detection scheme, which optimizes the result in terms of minimum BER. The second detection method, MRC, is based on linear combining technique and is optimal in the sense of maximizing the output SNR. It also includes an ML detection metric to minimize the BER of the combiner output. The third detection method exploits the ubiquitous linear MMSE detection technique, which provides an optimal solution for minimizing the error.

Motivated by the shortcomings of the existing detection techniques, the proposed detection schemes aim to deliver a near optimal solution for detection of the transmitted signal in the presence of both channel and CFO estimation error, for various estimation error variances of the uncertainties, which are presented in Chapter 5. The proposed algorithms aim to augment the three prevalent detection techniques that are used practically. The system model is proposed for a two transmit one receive antenna, which is extended to m -transmit antennas. It is also mathematically shown, that for ideal cases with perfect knowledge of channel and CFO, the proposed algorithms generalize and converge to their respective classical forms. At the end, a brief discussion is done on the computational complexities of the proposed detectors from the implementation point of view.

Extensive simulation results demonstrate that the proposed schemes outperform conventional detectors. The performance is analyzed by plotting the BER over SNR curves for various modulation schemes, such as 4, 8 and 16-PSK and 4, 16 and 64-QAM. The simulation graphs demonstrate that the proposed schemes yields an improved performance under the mismatch scenario and at higher error variances. Thus, it can be concluded that the proposed detection algorithms are a novel approach for practical implementation.

The system model considered in this thesis is a simple general case of a MISO system. The work presented here can be further extended for more complicated cases like multi-user MISO system using multiple detections, as in today's wireless LTE-4G system. Another future enhancement can be, implementation of the proposed detectors on MIMO systems for different modulation schemes, such as OFDMA, which is used practically in LTE advanced. OFDMA is used in downlink systems and faces the major challenges of Inter Channel and Inter Carrier Interference with mitigation of CFO. Apart from that, a similar approach for deriving detection algorithms conditioned on imperfect estimates can be implemented in combination with channel decoding. These three approaches are considered as a future enhancement to this research.

References

- [1] S. Sharma, *Communication systems (analog and digital)*, S K Kataria and sons, 2009.
- [2] G. Forney Jr., R. Gallager, G. Lang, F. Longstaff, and S. Qureshi, “Efficient modulation for band-limited channels,” *IEEE Journal on Selected Areas of Communications*, vol. 2, no. 5, pp. 632–647, Sep. 1984.
- [3] M. Kumar, S. Tripathi, A. Vidyarathi, S. Mohanty, and R. Gowri, “Various PSK modulation schemes for wireless communication,” *2nd International Conference on Computer and Communication Technology (IC CCT)*, pp. 545–549, Sep. 2011, 15-17.
- [4] H. Roder, “Amplitude, phase, and frequency modulation,” *Proceedings of the Institute of Radio Engineers*, vol. 19, no. 12, pp. 2145–2176, Dec. 1931.
- [5] W. T. Webb and R. Steele, “Variable rate QAM for mobile radio,” *IEEE Transactions on Communications*, vol. 43, no. 7, pp. 2223–2230, July 1995.
- [6] T. Le-Ngoc, G. M. Lieu, and V. K. Bhargava, “Performance of m-ary qam schemes in a line-of-sight multipath fading channel,” in *Proc. IEEE Pacific RIM Conference on Communications, Computers and Signal Process*, pp. 396–399, June 1989.
- [7] T. Xiaoyi, M. S. Alouini, and A. J. Goldsmith, “Effect of channel estimation error on M-QAM BER performance in rayleigh fading,” *IEEE Transactions on Communications*, vol. 47, no. 12, pp. 1856–1864, Dec. 1999.

- [8] T. P. Surekha, T. Ananthapadmanabha, and C. Puttamadappa, "Modeling and performance analysis of QAM-OFDM system with AWGN channel," *Third Pacific-Asia Conference on Circuits, Communications and System (PACCS)*, pp. 1–4, July 2011, 17-18.
- [9] N. Moezzi-Madani, T. Thorolfsson, J. Crop, P. Chiang, and W. R. Davis, "An energy-efficient 64-QAM MIMO detector for emerging wireless standards," *Design, Automation & Test in Europe Conference & Exhibition (DATE)*, 2011.
- [10] A. Mraz and L. Pap, "General interference analysis of M-QAM transmission applied to LTE performance evaluation," *EUROCON - IEEE International Conference on Computer as a Tool*, pp. 1–4, Apr. 2011, 27-29.
- [11] H. B. Voelcke, "Phase-shift keying in fading channels," *Journal of the Institution of Electrical Engineers*, vol. 6, no. 61, pp. 37, Jan. 1960.
- [12] O. Shimbo, R. Fang, and M. Celebiler, "Performance of M-ary PSK systems in gaussian noise and intersymbol interference," *IEEE Transactions on Information Theory*, vol. 19, no. 1, pp. 44–58, Jan. 1973.
- [13] J. B. Anderson, C-E. Sundberg, T. Aulin, and N. Rydbeck, "Power-bandwidth performance of smoothed phase modulation codes," *IEEE Transactions on Communications*, vol. 29, no. 3, pp. 187–195, Mar. 1981.
- [14] C. Tellambura, A. J. Mueller, and V. K. Bhargawa, "Analysis of M-ary phase-shift keying with diversity reception for land-mobile satellite channels," *IEEE Transactions on Vehicular Technology*, vol. 46, no. 4, pp. 910–922, Nov. 1997.
- [15] J. R. Edwards, "A comparison of modulation schemes for binary data transmission," *Radio and Electronic Engineer*, vol. 43, no. 9, pp. 562–568, Sep. 1973.
- [16] J. Oetting, "A comparison of modulation techniques for digital radio," *IEEE Transactions on Communications*, vol. 27, no. 12, pp. 1752–1762, Dec. 1979.

- [17] M. Tan and W. Chen, "Performance comparison and analysis of PSK and QAM," *7th International Conference on Wireless Communications, Networking and Mobile Computing (WiCOM)*, pp. 1–4, Sep. 2011, 23-25.
- [18] E. Ozturk and Y. Tunckaya, "Performances of M-PSK and M-QAM modulated OFDM signals over AWGN and rayleigh fading channels," *IEEE 18th Signal Processing and Communications Applications Conference (SIU)*, pp. 523–562, Apr. 2010, 22-24.
- [19] N. Srivastava, "Diversity schemes for wireless communication-a short review," *Journal on Theoretical and Application Information Technology*, vol. 15, no. 2, pp. 134–143, May 2010.
- [20] L. Zheng and D. N. C. Tse, "Diversity and multiplexing: a fundamental tradeoff in multiple-antenna channels," *IEEE Transactions on Information Theory*, vol. 49, no. 5, pp. 1073–1096, May 2003.
- [21] J. H. Winters, "Increased data rates for communication systems with adaptive antennas," in *Proc. IEEE International Conference of Communications*, June 1982.
- [22] J. H. Winters, J. Salz, and R. D. Gitlin, "The impact of antenna diversity on the capacity of wireless communication systems," *IEEE Transactions on Communications*, vol. 42, no. 234, pp. 1740–1751, Feb-Apr. 1994.
- [23] J. Salz and J. H. Winters, "Effect of fading correlation on adaptive arrays in digital mobile radio," *IEEE Transactions on Vehicular Technology*, vol. 43, no. 4, pp. 1049–1057, Nov. 1994.
- [24] D. G. Brennan, "On the maximal signal-to-noise ratio realizable from several noisy signals," *Proceedings IRE*, vol. 43, no. 10, pp. 1530, 1955.
- [25] D. G. Brennan, "Linear diversity combining techniques," *Proceedings IRE*, vol. 47, pp. 1075–1102, Jun 1959.

- [26] W. C. Jakes, "Microwave mobile communications," *Wiley, New York*, 1974.
- [27] R. A. Monzingo and T. W. Miller, "Introduction to adaptive arrays," *Wiley, New York*, 1980.
- [28] H. Jafarkhani, "Space-time coding: Theory and practice," *Cambridge University Press*, 2005.
- [29] S. M. Alamouti, "A simple transmit diversity technique for wireless communications," *IEEE Journal on Selected Areas of Communications*, vol. 16, pp. 1451–1458, Oct. 1998.
- [30] V. Weerackody, "Diversity for direct-sequence spread spectrum using multiple transmit antennas," in *Proceedings IEEE International Communication Conference*, pp. 1775–1779, May 1993.
- [31] B. Hochwald, T. L. Marzetta, and C. B. Papadias, "A transmitter diversity scheme for wideband CDMA systems based on space-time spreading," *IEEE Journal on Selected Areas of Communication*, vol. 19, no. 1, pp. 48–60, Jan. 2001.
- [32] V. M. Boachev and I. G. Kiselev, "Optimum combining of signals in space-diversity reception," *Telecommunications and Radio Engineering*, vol. 34/35, pp. 83, Oct. 1980.
- [33] J. H. Winters, "Smart antennas for wireless systems," *IEEE Personal Communications*, vol. 5, no. 1, pp. 23–27, Feb. 1998.
- [34] A. J. Paulraj, D. A. Gore, R. U. Nabar, and H. Bolcskei, "An overview of MIMO communications - a key to gigabit wireless," *Proceedings of the IEEE*, vol. 92, no. 2, pp. 198–218, Feb. 2004.
- [35] E. Telatar, "Capacity of multi-antenna gaussian channels," *European Transactions on Telecommunications*, vol. 10, no. 6, pp. 585–595, Nov-Dec. 1999.

- [36] S. Cui, A. J. Goldsmith, and A. Bahai, “Energy-efficiency of MIMO and cooperative MIMO in sensor networks,” *IEEE Journal on Selected Areas of Communications*, vol. 22, no. 6, pp. 1089–1098, Aug. 2004.
- [37] H. Bai and M. Atiquzzaman, “Error modeling schemes for fading channels in wireless communications: A survey,” *IEEE Communications Surveys & Tutorials*, vol. 5, no. 2, pp. 2–9, Quarter 2003.
- [38] B. Sklar, “Rayleigh fading channels in mobile digital communication systems part i: Characterization,” *IEEE Communication Magazine*, vol. 35, no. 11, pp. 90–100, July 1997.
- [39] M. Jankiraman, “Space-time codes and MIMO systems,” *Artech House*, Aug. 2004.
- [40] R.D. Yates and D.J. Goodman, “Probability and stochastic processes a friendly introduction for electrical and computer engineers,” *John Wiley and Sons, Inc.*, 2005.
- [41] J. H. Winters, “Optimum combining in digital mobile radio with co channel interference,” *IEEE Transactions on Vehicular Technology*, vol. 33, no. 3, pp. 144–155, Aug. 1984.
- [42] J. Salz, “Digital transmission over cross-coupled linear channels,” *AT&T Technical Journal*, vol. 64, no. 6, pp. 1147–1159, July-Aug. 1985.
- [43] G. J. Foschini, “Layered space-time architecture for wireless communications in a fading environment when using multi-element antennas,” *Bell Labs Technical Journal*, vol. 1, pp. 41–59, Autumn 1996.
- [44] G. J. Foschini and M. J. Gans, “Limits of wireless communications in a fading environment when using multiple antennas,” *Wireless Personal Communications*, vol. 6, pp. 311–335, Jan. 1998.

- [45] J. Guey, M. P. Fitz, M. R. Bell, and W. Kuo, "Signal design for transmitter diversity wireless communication systems over rayleigh fading channels," in *Proc. IEEE Vehicular Technology Conference*, vol. 1, pp. 136–140, 1996.
- [46] A. Narula, M. D. Trott, and G. W. Wornell, "Information-theoretic analysis of multiple-antenna transmission diversity," in *Proc. International Symposium on Information Theory and its Applications*, Sep. 1996.
- [47] N. Seshadri and J. H. Winters, "Two signaling schemes for improving the error performance of frequency division duplex (FDD) transmission systems using transmitter antenna diversity," *International Journal of Wireless Information Networks*, vol. 1, no. 1, pp. 49–60, Jan. 1994.
- [48] G. W. Wornell and M. D. Trott, "Efficient signal processing techniques for exploiting transmit antenna diversity on fading channels," *IEEE Transaction on Signal Processing*, vol. 45, pp. 191–205, 1997.
- [49] A. F. Naguib, A. Paulraj, and T. Kailath, "Capacity improvement with base-station antenna arrays in cellular CDMA," *IEEE Transactions on Vehicular Technology*, vol. 43, no. 3, pp. 691–698, Aug. 1994.
- [50] E. Biglieri, G. Taricco, and A. Tulino, "Performance of space-time codes for a large number of antennas," *IEEE Transactions on Information Theory*, vol. 48, no. 7, pp. 1794–1803, July 2002.
- [51] V. Tarokh, N. Seshadri, and A. R. Calderbank, "Space-time codes for high data rate wireless communication: Performance criterion and code construction," *IEEE Transaction of Information Theory*, vol. 44, pp. 744–765, Mar. 1998.
- [52] G. Ungerboeck, "Trellis-coded modulation with redundant signal sets part I: introduction," *IEEE Communications Magazine*, vol. 25, no. 2, pp. 5–11, 1987.

- [53] H. Jafarkhani, "A quasi-orthogonal space-time block code," *IEEE Transactions on Communications*, vol. 49, no. 1, pp. 1–4, Jan. 2001.
- [54] V. Tarokh, H. Jafarkhani, and A. R. Calderbank, "Space-time block codes from orthogonal designs," *IEEE Transactions on Information Theory*, vol. 45, no. 5, pp. 1456–1467, July 1999.
- [55] A. Scaglione, P. Stoica, S. Barbarossa, G. B. Giannakis, and H. Sampath, "Optimal designs for space-time linear precoders and decoders," *IEEE Transactions on Signal Processing*, vol. 50, no. 5, pp. 1051–1064, May 2002.
- [56] B. Hassibi and B. M. Hochwald, "High-rate codes that are linear in space and time," *IEEE Transactions on Information Theory*, vol. 48, no. 7, pp. 1804–1824, July 2002.
- [57] V. Tarokh, A. Naguib, N. Seshadri, and A. R. Calderbank, "Space-time codes for high data rate wireless communication: performance criteria in the presence of channel estimation errors, mobility, and multiple paths," *IEEE Transaction on Communication*, vol. 47, no. 2, pp. 199–207, Feb. 1999.
- [58] S. Sun and Y. Jing, "Channel training design in amplify-and-forward MIMO relay networks," *IEEE Transaction on Wireless Communication*, vol. 10, no. 10, pp. 3380–3391, Oct. 2011.
- [59] T. M. Schmidl and D. C. Cox, "Robust frequency and timing synchronization for OFDM," *IEEE Transactions on Communications*, vol. 45, no. 12, pp. 1613–1621, 1997.
- [60] P. H. Moose, "A technique for orthogonal frequency division multiplexing frequency offset correction," *IEEE Transactions on Communications*, vol. 42, no. 10, pp. 2908–2914, Oct. 1994.

- [61] L. Rugini, P. Banelli, H. A. Suraweera, and C. Yuen, "Performance of alamouti space-time coded OFDM with carrier frequency offset," *IEEE Global Telecommunications Conference*, pp. 1–5, Dec. 2011.
- [62] T.M. Mingqian, A.S. Madhukumar, A.B. Premkumar, and E.M.-K. Lai, "Frequency offset correction for space-time block coded OFDM systems based on maximum likelihood estimation," *Proceedings of the 2003 Joint Conference of the Fourth International Conference on Information, Communications and Signal Processing, 2003 and the Fourth Pacific Rim Conference on Multimedia.*, vol. 2, pp. 926–929, Dec. 2003.
- [63] J. Mietzner, R. Schober, L. Lampe, W. H. Gerstacker, and P. A. Hoeher, "Multiple-antenna techniques for wireless communications - a comprehensive literature survey," *IEEE Communications Surveys Tutorials*, vol. 11, no. 2, pp. 87–105, quarter 2009.
- [64] M. Krondorf, T. J. Liang, and G. Fettweis, "Symbol error rate of OFDM systems with carrier frequency offset and channel estimation error in frequency selective fading channels," in *Proceedings IEEE International Communication Conference*, pp. 5132–5136, June 2007.
- [65] Z. Zhang and C. Tellambura, "The effect of imperfect carrier frequency offset estimation on an OFDMA uplink," *IEEE Transactions on Communications*, vol. 57, pp. 1025–1030, April 2009.
- [66] F. Gini and G. B. Giannakis, "Frequency offset and symbol timing recovery in flat-fading channels: a cyclostationary approach," *IEEE Transaction on Communication*, vol. 46, no. 3, pp. 400411, Mar. 1998.
- [67] T. Wo, J. C. Fricke, and P. A. Hoeher, "A graph-based iterative gaussian detector for frequency-selective MIMO channels," in *Proceedings IEEE Information Theory Workshop*, pp. 581–585, Oct. 2006.

- [68] X. Zhu and R. D. Murch, "Performance analysis of maximum likelihood detection in a MIMO antenna system," *IEEE Transactions on Communications*, vol. 50, no. 2, pp. 187–191, Feb. 2002.
- [69] W. Peng, M. Shaodan, Tung-Sang Ng, W. Jiangzhou, and F. Adachi, "Performance analysis on maximum likelihood detection for two input multiple output systems," in *Proceedings IEEE Vehicular Technology.*, pp. 1–5, Sept. 2008.
- [70] G. V. V. Sharma and A. Chockalingam, "Performance analysis of maximum-likelihood multiuser detection in space-time coded CDMA with imperfect channel estimation," in *Proceedings IEEE Vehicular Technology*, pp. 1664–1668, May 2004.
- [71] M. Kiessling, J. Speidel, N. Geng, and M. Reinhardt, "Performance analysis of MIMO maximum likelihood receivers with channel correlation, colored gaussian noise, and linear prefiltering," in *Proceedings IEEE International Conference on Communication*, pp. 3026–3030, May 2003.
- [72] S. S. Dragomir, "A survey on cauchy-bunyakovsky-schwarz type discrete inequalities," *Journal of Inequalities in Pure and Applied Mathematics*, vol. 4, no. 3, pp. 63, May 2003.
- [73] A. H. Sayed, "Fundamentals of adaptive filtering," *John Wiley and Sons*, 2003.
- [74] K. Namshik, L. Yusung, and H. Park, "Performance analysis of MIMO system with linear MMSE receiver," *IEEE Transaction on Wireless Communication*, vol. 7, no. 11, pp. 4474–4478, Nov. 2008.
- [75] H. V. Poor and S. Verdu, "Probability of error in MMSE multiuser detection," *IEEE Transaction on Information Theory*, vol. 43, no. 3, pp. 858–871, May 1997.
- [76] Li-Chung Chu and U. Mitra, "Performance analysis of an improved MMSE multiuser receiver for mismatched delay channels," *IEEE Transaction on Communication*, vol. 46, no. 10, pp. 1369–1380, Oct. 1998.

- [77] H. Li and H. V. Poor, "Impact of imperfect channel estimation on turbo multiuser detection in DS-CDMA systems," in *Proceedings IEEE Wireless Communication Network*, pp. 30–35, Mar. 2004.
- [78] B. Xia, J. Wang, and M. Sawahashi, "Performance comparison of optimum and MMSE receivers with imperfect channel estimation for VSF-OFCDM systems," *IEEE Transaction on Wireless Communication*, vol. 4, no. 6, pp. 3051–3062, Nov. 2005.
- [79] V. Tarokh, A. Naguib, N. Seshadri, and A. R. Calderbank, "Space-time codes for high data rate wireless communication: performance criteria in the presence of channel estimation errors, mobility, and multiple paths," *IEEE Transaction on Communication*, vol. 47, no. 2, pp. 199–207, Feb 1999.
- [80] B. Morshed and B. Shahrrava, "A new metric for space-time block codes with imperfect channel estimates," in *Proceedings IEEE WiMob, Montreal, Canada*, pp. 174–181, Aug. 2005.
- [81] Y. Chen and N.C. Beaulieu, "Maximum likelihood receivers for space-time coded mimo systems with gaussian estimation errors," *IEEE Transaction on Communication*, vol. 57, no. 6, pp. 1712–1720, June 2009.

Appendix A

Mathematical Calculations

The proposed detection schemes derived in Chapter 5 utilizes some mathematical expressions and values, derived and calculated in this chapter. In section A.1, we introduce the initial assumptions made for CFO and derive the conditional PDF of CAFO with its estimate. Section A.2 derives the expected value of CAFO function conditioned on its estimates using the PDF in section A.1. These values are further used for calculating the expectation of the received signal conditioned on the imperfect estimates as given in section A.3 and variance of the received signal conditioned on imperfect estimates, derived in section A.4.

A.1 Conditional PDF of CAFO

CFO is a term used to represent the mismatch between the receiver oscillator frequency and carrier frequency of the transmitted signal which is given as

$$\Delta f = f_c - f_r$$

and the baseband signal transmitted from the i -th antenna and received at k -th instant with CFO is

$$r_k = \sqrt{E_s} \sum_{i=0}^{m-1} h_i s_{i,k} e^{j\phi_{i,k}} + n_k. \quad (\text{A.1})$$

Here, $\phi_{i,k}$ is the CAFO with a sampling frequency f_s

$$\phi_{i,k} = \frac{2\pi\Delta f_{i,k}}{f_s}.$$

Let us assume, that the CAFO $\phi_{i,k} \sim \mathcal{N}(0, \sigma_\phi^2)$ is a zero mean Gaussian RV with variance σ_ϕ^2 . It follows the distribution function given as

$$f_\phi(\phi_{i,k}) = \frac{1}{\sqrt{2\pi\sigma_\phi^2}} e^{\left(\frac{-\phi_{i,k}^2}{2\sigma_\phi^2}\right)}. \quad (\text{A.2})$$

The estimator of CAFO, regardless of its type is modeled as

$$\hat{\phi}_{i,k} = \phi_{i,k} + \epsilon_{i,k},$$

where the estimation error $\epsilon_{i,k} \sim \mathcal{N}(0, \sigma_\epsilon^2)$ is taken as a zero mean Gaussian RV having variance σ_ϵ^2 and thus it is evident that the CAFO estimate $\hat{\phi}_{i,k} \sim \mathcal{N}(0, \sigma_{\hat{\phi}}^2)$ is also a zero mean Gaussian RV with variance $\sigma_{\hat{\phi}}^2$. The original value of CAFO $\phi_{i,k}$ and its estimate $\hat{\phi}_{i,k}$ are dependent on each other by the correlation coefficient

$$\begin{aligned} \lambda &= \frac{E[\phi_{i,k}\hat{\phi}_{i,k}]}{\sqrt{\sigma_\phi^2\sigma_{\hat{\phi}}^2}} \\ &= \frac{E[\phi_{i,k}(\phi_{i,k} + \epsilon_{i,k})]}{\sqrt{\sigma_\phi^2\sigma_{\hat{\phi}}^2}} \\ &= \frac{\sigma_\phi^2}{\sqrt{\sigma_\phi^2\sigma_{\hat{\phi}}^2}} \quad \because \phi_{i,k} \perp \epsilon_{i,k} \\ &= \sqrt{1 - \frac{\sigma_\epsilon^2}{\sigma_{\hat{\phi}}^2}}. \end{aligned}$$

Using the relations for bi-variate Gaussian distributions given in standard literature, we get the expected value $\phi_{i,k}$ conditioned on $\hat{\phi}_{i,k}$ as

$$E[\phi_{i,k}|\hat{\phi}_{i,k}] = \frac{\lambda\sigma_{\phi_{i,k}}\hat{\phi}_{i,k}}{\sigma_{\hat{\phi}_{i,k}}} \quad (\text{A.3})$$

and the conditional variance as

$$\text{Var} \left[\phi_{i,k} | \hat{\phi}_{i,k} \right] = (1 - \lambda^2) \sigma_{\hat{\phi}_{i,k}}^2 \quad (\text{A.4})$$

With the above relations, it is easily shown that the conditional PDF of $\phi_{i,k}$ given $\hat{\phi}_{i,k}$ is

$$f_{\phi|\hat{\phi}} \left(\phi_{i,k} | \hat{\phi}_{i,k} \right) = \frac{1}{\sqrt{2\pi(1-\lambda^2)}} e^{-\frac{\left| \phi_{i,k} - \frac{\lambda \hat{\phi}_{i,k}}{\sigma_{\hat{\phi}_{i,k}}} \right|^2}{2(1-\lambda^2)}}. \quad (\text{A.5})$$

The above PDF will be used in the next chapter for further derivation.

A.2 Conditional Expectation of CAFO

In this section, the conditional expectation of the function of CAFO with the estimate is calculated. From the expression of baseband signal given in (A.1) and the PDF derived in (A.5), we can calculate

$$\begin{aligned} E \left[e^{j\phi_{i,k}} | \hat{\phi}_{i,k} \right] &= \int_{-\infty}^{\infty} e^{j\phi_{i,k}} f_{\phi|\hat{\phi}} \left(\phi_{i,k} | \hat{\phi}_{i,k} \right) d\phi \\ &= \int_{-\infty}^{\infty} \frac{e^{j\phi_{i,k}}}{\sqrt{2\pi(1-\lambda^2)}} e^{-\frac{\left| \phi_{i,k} - \frac{\lambda \hat{\phi}_{i,k}}{\sigma_{\hat{\phi}_{i,k}}} \right|^2}{2(1-\lambda^2)}} d\phi \end{aligned} \quad (\text{A.6})$$

Let $a = 2(1 - \lambda^2)$ and $b = \frac{\lambda \hat{\phi}_{i,k}}{\sigma_{\hat{\phi}_{i,k}}}$, thus the above equation becomes

$$E \left[e^{j\phi_{i,k}} | \hat{\phi}_{i,k} \right] = \frac{1}{\sqrt{a\pi}} \int_{-\infty}^{\infty} e^{j\phi_{i,k}} e^{-\frac{|\phi_{i,k} - b|^2}{a}} d\phi. \quad (\text{A.7})$$

Again, let $z = \phi_{i,k} - b \Rightarrow dz = d\phi$ and $\phi_{i,k} = z + b$.

$$\begin{aligned}
E \left[e^{j\phi_{i,k}} \mid \hat{\phi}_{i,k} \right] &= \frac{1}{\sqrt{a\pi}} \int_{-\infty}^{\infty} e^{j(z+b)} e^{(-z^2/a)} dz \\
&= \frac{e^{jb}}{\sqrt{a\pi}} \int_{-\infty}^{\infty} e^{jz} e^{(-z^2/a)} dz \\
&= e^{jb} e^{(-a/4)}.
\end{aligned} \tag{A.8}$$

Substituting the values of a and b

$$E \left[e^{j\phi_{i,k}} \mid \hat{\phi}_{i,k} \right] = e \left(\frac{j\lambda\hat{\phi}_{i,k} - (1 - \lambda^2)}{2\sigma_{\hat{\phi}_{i,k}}} \right). \tag{A.9}$$

A.3 Conditional Expectation of Received Signal

According to the assumptions made earlier in the thesis, the channel fading parameter $h_i \sim \mathcal{N}(0, 1)$ is a zero mean Gaussian RV with unit variance. The imperfect channel estimate $\hat{h}_i \sim \mathcal{N}(0, \sigma_{\hat{h}}^2)$, its estimation error $\varepsilon_i \sim \mathcal{N}(0, \sigma_{\varepsilon}^2)$ and the AWGN $n_k \sim \mathcal{N}(0, N_0)$ also follow Gaussian distribution with mean zero with variances $\sigma_{\hat{h}}^2$, σ_{ε}^2 and N_0 respectively. The correlation coefficient between h_i and \hat{h}_i is given as

$$\rho = \frac{1}{\sqrt{1 + \sigma_{\varepsilon}^2}}.$$

Here, the results given in [79] are directly used, which are as follows

$$\begin{aligned}
E \left[h_i \mid \hat{h}_i \right] &= \frac{\rho\hat{h}_i}{\sigma_{\hat{h}}} \\
Var \left[h_i \mid \hat{h}_i \right] &= 1 - \rho^2 \\
E \left[r_k \mid \hat{h}_i \right] &= \frac{\rho\hat{h}_i \sqrt{E_s} s_{i,k}}{\sigma_{\hat{h}}} \\
Var \left[r_k \mid \hat{h}_i \right] &= N_0 + (1 - \rho^2) E_s |s - i, k|^2.
\end{aligned} \tag{A.10}$$

Now, let us calculate the expected value of the received signal r_k conditioned on the channel estimate \hat{h}_i and the CFO estimate $\hat{\phi}_{i,k}$. Thus from (A.1) and (A.9),

$$\begin{aligned} E \left[r_k \mid \hat{h}_i, \hat{\phi}_{i,k} \right] &= \sqrt{E_s s_{i,k}} E \left[h_i \mid \hat{h}_i \right] E \left[e^{j\phi_{i,k}} \mid \hat{\phi}_{i,k} \right] \\ &= \frac{\rho \hat{h}_i}{\sigma_{\hat{h}}} \sqrt{E_s s_{i,k}} e^{\left(\frac{j\lambda \hat{\phi}_{i,k}}{\sigma_{\hat{\phi}_{i,k}}} - \frac{(1-\lambda^2)}{2} \right)}. \end{aligned} \quad (\text{A.11})$$

Let us consider the parameter introduced in (4.20)

$$x_{i,k} = h_i e^{j\phi_{i,k}}.$$

We can calculate the expectation of $x_{i,k}$ conditioned on \hat{h}_i and $\hat{\phi}_{i,k}$ as

$$\begin{aligned} E \left[x_{i,k} \mid \hat{h}_i, \hat{\phi}_{i,k} \right] &= E \left[h_i \mid \hat{h}_i \right] E \left[e^{j\phi_{i,k}} \mid \hat{\phi}_{i,k} \right] \\ &= \frac{\rho \hat{h}_i}{\sigma_{\hat{h}}} e^{\left(\frac{j\lambda \hat{\phi}_{i,k}}{\sigma_{\hat{\phi}_{i,k}}} - \frac{(1-\lambda^2)}{2} \right)}. \end{aligned} \quad (\text{A.12})$$

A.4 Conditional Variance of Received Signal

In the section, the aim is to calculate the variance of received signal r_k conditioned on the channel estimate \hat{h}_i and the CFO estimate $\hat{\phi}_{i,k}$. To obtain this, we need to do some preliminary calculations. Using (A.10), it can be easily written

$$\begin{aligned} E \left[|h_i|^2 \mid \hat{h}_i \right] &= \text{Var} \left[h_i \mid \hat{h}_i \right] + \left(E \left[h_i \mid \hat{h}_i \right] \right)^2 \\ &= 1 - \rho^2 + \frac{\rho^2 \left| \hat{h}_i \right|^2}{\sigma_{\hat{h}}^2}. \end{aligned} \quad (\text{A.13})$$

We can easily say from the relation of $x_{i,k}$,

$$E \left[|x_{i,k}|^2 \mid \hat{h}_i, \hat{\phi}_{i,k} \right] = E \left[|h_i|^2 \mid \hat{h}_i \right].$$

Now, we calculate the second moment of the received signal r_k conditioned on \hat{h}_i and $\hat{\phi}_{i,k}$

$$\begin{aligned} E \left[|r_k|^2 \mid \hat{h}_i, \hat{\phi}_{i,k} \right] &= E \left[|h_i|^2 \mid \hat{h}_i \right] E_s |s_{i,k}|^2 + \sigma_n^2 \\ &= \left(1 - \rho^2 + \frac{\rho^2 \left| \hat{h}_i \right|^2}{\sigma_{\hat{h}}^2} \right) E_s |s_{i,k}|^2 + N_0. \end{aligned} \quad (\text{A.14})$$

Using the above result and from (A.11), we can easily calculate the variance of r_k conditioned on \hat{h}_i and $\hat{\phi}_{i,k}$

$$\begin{aligned} Var \left[r_k \left| \hat{h}_i, \hat{\phi}_{i,k} \right. \right] &= E \left[|r_k|^2 \left| \hat{h}_i, \hat{\phi}_{i,k} \right. \right] - \left(E \left[r_k \left| \hat{h}_i, \hat{\phi}_{i,k} \right. \right] \right)^2 \\ &= N_0 + E_s |s_{i,k}|^2 (1 - \rho^2) + \left(1 - e^{(\lambda^2 - 1)} \right) \frac{\rho^2 E_s |s_{i,k}|^2 \hat{h}_i^2}{2\sigma_h^2}. \end{aligned} \quad (\text{A.15})$$

Vita Auctoris

NAME : Garima Deep

BIRTH YEAR : 1987

BIRTH PLACE : INDIA

EDUCATION

2010–2012 : **Masters of Applied Science**

Electrical and Computer Engineering

University of Windsor, Windsor, Ontario, Canada

2005–2009 : **Bachelor of Technology**

Electronics and Communications Engineering

Guru Tegh Bahadur Institute of Technology,

GGSIPIU, Delhi, India